Functional traits of three *Ulmus minor* fungal endophytes and their role in host resistance to *Ophiostoma novo-ulmi*

Footnote to the title: Elm endophytes and Dutch elm disease resistance

Martínez-Arias, C[1]; Sobrino-Plata, J[1]; Ormeño-Moncalvillo, S[1]; Gil, L[1]; Rodríguez-Calcerrada, J[1] and Martín, JA[1*].

[1] Departamento de Sistemas y Recursos Naturales, ETSI Montes, Forestal y del Medio Natural, Universidad Politécnica de Madrid, Madrid, 28040 Spain

*Author for correspondence: *Juan Antonio Martín García*. *Tel: +34 910671758*. *Email: juan.martin.garcia@upm.es*

Abstract:

Certain fungal endophytes are known to improve plant resistance to biotic stresses in forest trees. In this study, three stem fungal endophytes belonging to classes Cystobasidiomycetes, Eurotiomycetes and Dothideomycetes were selected among 210 isolates for their potential as enhancers of *Ulmus minor* resistance to *Ophiostoma novo-ulmi*. We evaluated phenotypic traits of these endophytes that could be beneficial for *O. novo-ulmi* inhibition in the host plant. Under *in vitro* conditions, the Dothideomycetous isolate YCB36 strongly inhibited *O. novo-ulmi* growth, released antipathogen VOCs, chitinases and siderophores, and overlapped with the pathogen in nutrient utilization patterns. These functional traits could explain the 40% reduction in leaf wilting due to *O. novo-ulmi* in elm trees pre-inoculated with this endophyte. *Ulmus minor* trees responded to endophyte inoculation with increased stomatal conductance and higher amounts of flavonoids and total phenolic compounds in xylem tissues, suggesting induction of defence metabolism.

Keywords: antibiosis, biocontrol, Cystobasidium, Dutch elm disease, resistance, Dothideomycetes, elm, endotherapy, Exophiala, fungal endophytes.

Introduction

In natural ecosystems, plants host a broad spectrum of microbes, especially fungi and bacteria that can colonize the plant surface as epiphytes or inner plant tissues as endophytes. When living inside plants, some endophytes act as mutualistic symbionts, assisting plant functioning, survival and fitness (Carroll, 1988; Hardoim et al., 2015). Fungal endophytes have received considerable attention in recent years because of their impact on plant fitness (Lata et al., 2018; Rodriguez et al., 2009) and plant responses to biotic and abiotic stressors. Fungi have been associated with plants for at least 400 million years, and facilitated their adaptation to land (Krings et al., 2007). The role of fungal endophytes in plant resilience is especially important in trees, which face extreme weather conditions and recurring pathogen and insect attacks during their long lifespan.

Abiotic stress resistance conferred by symbiotic microorganisms involves plant modifications that lead to improved nutrient acquisition (Malinowski and Beleski, 2000; Almario et al., 2017), plant physiological or molecular responses to the stress (Redman et al., 2011; Dastogeer et al., 2018; Redman et al., 1999), and enhanced plant growth (Vinale et al., 2008; Khan et al., 2009). Endophytic fungi can shape host resistance to biotic stressors through several mechanisms (Gao et al., 2010; Witzell and Martín, 2018). Some of these are based on direct interaction between endophytes and pathogens, such as mycoparasitism, competitive exclusion by substrate consumption, and inhibition of the pathogen by extracellular chemicals released by the endophyte, e.g. by proteases or chitinases, which are able to degrade the hyphal cell wall of pathogens (dos Reis Almeida et al., 2007; Guthrie and Castle, 2006; Orlandelli et al., 2015). Indirectly, endophytes can stimulate the defensive response of the plant through alterations of defence transduction pathways (Khare et al., 2018; Fesel and Zuccaro, 2016). Some endophytes enhance plant growth by synthesizing gibberellins (e.g. gibberellic acid, GA_3) and auxins (e.g. indole-3-acetic acid, IAA) (Patten and Glick, 2002; Shi et al., 2009; Videira et al., 2012) or by improving nutrient acquisition, helping to counteract the negative effects of pathogen invasion.

Phosphate solubilization (Oteino et al., 2015; Passari et al., 2015), siderophore emission (Bartholdy et al., 2001; Radzki et al., 2013) and hydrogen cyanide (HCN) production (Haas and Defago, 2005) are the main mechanisms provided by symbionts to improve plant nutrient uptake. Siderophores and HCN have also been reported to aid biological control of plant pathogens by acting as antimicrobial compounds (Verma et al., 2011; Senthilkumar et al., 2009; Haselwandter et al., 2007; Rijavec and Lapanje, 2016). Endophyte-induced oxidative stress could enhance synthesis of plant antioxidant molecules and increase oxidative protection from biotic and abiotic stressors (White and Torres, 2010). Flavonoids and other phenolic antioxidants are some of the main molecules involved in these processes (Yang et al., 2016).

In recent decades, interest has increased in the study of fungal endophytes and their use as biological control agents (Arnold et al., 2003; Mejía et al., 2008; Fakhro et al., 2010; Martínez-Álvarez et al., 2016; Martínez-Arias et al., 2018; Rabiey et al., 2019; Halecker et al., 2020). Locally adapted endophytes and easily cultured strains are desirable in successful use of endophytes as biocontrol agents. Using local endophytes reduces the risk of incompatible interactions with the host plant and adverse environmental conditions for fungal development, while easily cultured endophytes facilitate inoculum production. Multi-species microbial consortia can provide better results than single species due to the wider array of complex functions they perform (Brenner et al., 2008). However, it is necessary to study a single species or a consortium of a few species as a first step to evaluate specific functions and effects. The vast fungal diversity hosted in plant tissues obliges researchers to pre-select fungi with the greatest potential for providing plant health benefits, e.g. by using *in vitro* tests. Greater understanding of the ecology and behaviour of fungal endophytes in host plants is likely to boost their use in plant disease management or breeding programmes through microbial community engineering. Some of the main strategies proposed to selectively modify, increase or sustain certain microbial communities include amending soil with beneficial organisms, inoculating plants or seeds with beneficial organisms

before planting, and maintaining structural heterogeneity and potentially diverse habitats and substrates (Witzell and Martín 2018).

Dutch elm disease (DED), introduced into Europe and North America by global trade in the first half of the 20th century, was one of the earliest examples of alien diseases threatening native forests. The current DED pandemic was caused by *Ophiostoma novo-ulmi* Brasier (Sordariomycetes), which is transmitted into healthy elm trees through bark beetles of the genera *Scolytus* and *Hylurgopinus*. *O. novo-ulmi* spreads within xylem vessels, causing blockage and embolism (Brasier and Buck, 2001; Martín et al., 2019). Among the various biocontrol agents studied to reduce the impact of DED (Schelfer et al., 1990; Solla and Gil, 2003), fungal endophytes have received increasing attention in recent years (Blumenstein et al., 2015; Martín et al., 2013; Martín et al., 2015). In elms, distinct fungal assemblages were found in the xylem of susceptible and tolerant genotypes (Martín et al., 2013). Some of these endophytes were isolated and tested against *O. novo-ulmi in vitro* and in field plot assays (Martín et al., 2015), and some showed the ability to reduce DED symptoms. However, environmental factors and host genotype appeared to alter the behaviour and spread of the inoculated fungi, providing an unstable protective effect (Martín et al, 2015).

In this work, we aimed to explore the functional mechanisms used by fungal endophytes to increase host resistance against pathogens, using the DED complex as a case study. We selected three fungal endophytes from a collection of 210 isolates following two criteria. The first criterion was based on earlier metabarcoding research by our group that revealed a close association between the abundance of operational taxonomic units within classes Cystobasidiomycetes and Eurotiomycetes and the level of host resistance to DED (Macaya-Sanz et al., unpublished results). In light of this result, we hypothesize that elm endophytes belonging to these fungal classes exhibit functional traits involved in *U. minor* resistance to DED. The second criterion was based on other research showing that although most endophytes are able

to reduce the growth of *O. novo-ulmi* in *in vitro* dual tests to some extent, only a few endophytes are able to strongly inhibit pathogen growth by antibiosis mechanisms (Martín et al., 2015). Release of extracellular antifungal compounds into the culture medium and emission of antifungal volatile organic compounds (VOCs) may be responsible for this strong inhibition (Blumenstein et al., 2015). Therefore, we further hypothesize that fungal endophytes exhibiting strong antibiotic activity towards *O. novo-ulmi* have the potential to reduce *O. novo-ulmi* spread *in planta* and consequently decrease disease symptoms.

According to the former general aim and hypothesis, we evaluated several phenotypic traits of two endophytes representative of classes Cystobasidiomycetes and Eurotiomycetes, and an additional Dothideomycetous isolate which showed strong *in vitro* antibiosis towards *O. novo-ulmi* in preliminary screening tests. Our four objectives were to: i) characterize *in vitro* the type of interaction and the antibiotic potential of the three selected endophytes against *O. novo-ulmi*, ii) determine the nutrient metabolism, nutrient uptake ability and production of plant growth-promoting compounds by the endophytes, iii) evaluate the plant colonization ability of the endophytes and their protective effect against *O. novo-ulmi* in a field assay with 6-year-old susceptible *U. minor* trees, and iv) study the plant functional and chemical response to the endophytes to explain the protective effect against the pathogen.

Material and methods

Fungal material

Three fungal endophytes isolated from elm twigs and named YM11, P5 and YCB36 were selected for the experiments. The endophytes are from a collection of fungi that includes 210 isolates obtained from *U. minor* trees in the last 10 years, conserved by the Spanish elm breeding programme. The three selected fungi were isolated in 2014 and 2015 from three *U. minor* genotypes tolerant to DED (Martín et al., 2015) growing in a conservation plot at Puerta de Hierro Forest Breeding Centre, Madrid (Spain, 40° 27’ 24’’ N; 3° 45’ 0’’ W; 600 m. a.s.l.). YM11

and P5 isolates can be morphologically classified as black and pink yeasts, respectively, and were selected because they belong to Eurotiomycetes and Cystobasidiomycetes, two fungal classes with high resistance to *O. novo-ulmi* commonly occurring in *U. minor* trees (Macaya-Sanz et al., unpublished results). YM11 colonies growing in standard culture medium comprise a mixture of bud cells and hyphae, while P5 forms bud cell aggregates. Additionally, the YCB36 isolate, a filamentous fungus within Dothideomycetes, was selected because it strongly inhibited *O. novo-ulmi* growth in preliminary *in vitro* screening tests (visual assessment). This fungus produces a dark halo around the colony when grown on 3.5 % yeast extract agar (YEA), indicating release of metabolites that could cause inhibition in *O. novo-ulmi* growth.

After initial isolation on 3.5% YEA, 4 × 4 mm plugs of each endophyte isolate were conserved in sterilized distilled water (dH_2O) at 4 ^oC in the dark. Two months before the experiment, isolates were sub-cultured on 3.5% YEA in the dark at 22 ^oC. These colonies were subcultured every 15 days to fresh YEA petri dishes and used as stock source for subsequent assays. For molecular identification of endophytes, isolates were grown on YEA medium over an autoclaved cellophane layer. Five hundred milligrams of the mycelium were harvested and ground with a pellet pestle. DNA extraction was carried out as described by Martínez-Arias et al. (2018). After DNA extraction, the two Internal Transcribed Spacers (ITS) of ribosomal DNA were amplified through Polymerase Chain Reaction (PCR) for each fungal strain using universal primers ITS1F (5'-CTTGGTCATTTAGAGGAAGTAA-3') and ITS4 (5'-TCCTCCGCTTATTGATATGC-3'), following a protocol based on White and Bruns (1990). The amplification product was Sanger-sequenced, and sequences were annotated taxonomically based on the most similar sequence with taxonomic identity using the Genbank Basic Local Alignment Search Tool (BLASTn) of the National Centre for Biotechnology Information database (NCBI, MD, USA).

The *O. novo-ulmi* ssp. *americana* isolate SOM-1 was used in the experiments (Martín et al., 2019). It was isolated in 2014 from a 168-year-old *U. minor* tree in El Pardo (Madrid, Spain) and

had *in vitro* growth of 4 mm per day on 2% malt extract agar (MEA) at 20 °C. The identity of the pathogen was determined by assessments of colony morphology and growth rates at 20 °C and 33 °C, according to Brasier (1981). To confirm species and subspecies identity, a molecular analysis of the isolate was performed according to Gibb and Hausner (2005), as described in Martín et al. (2019). The isolate was conserved as mycelial plugs immersed in sterilized dH_2O and subcultured on 2% MEA two months before the experiment, kept in the dark at 22 °C, and subcultured every 15 days.

In vitro characterization of fungal endophytes

Dual culture with O. novo-ulmi

Each endophyte was co-cultured with *O. novo-ulmi* in the same petri dish. Mycelial plugs (5 x 5 mm) of both the endophyte and the pathogen were subcultured from the actively growing colony edge and transferred to new dishes with 3.5% YEA. *Ophiostoma novo-ulmi* and endophyte plugs were spaced 4 cm apart in the petri dish. In control plates, *O. novo-ulmi* was confronted against itself. Colony growth was measured at 3, 7, 10 and 12 days of incubation by scanning the growth area of each fungus using ImageJ software (http://imagej.nih.gob/ij/). Relative growth inhibition of *O. novo-ulmi* by endophytes was calculated by comparing *O. novo-ulmi* colony growth in control plates and endophyte-confronted plates (Chamberlain and Crawford, 1999; Kusari et al., 2013). Interaction between the endophyte and the pathogen was also assessed qualitatively according to Mejía et al. (2008): i) antibiosis (the endophyte is able to reduce pathogen growth by the release of antifungal compounds without mycelial contact between the two colonies, and a halo is usually observed), ii) mycoparasitism (the endophyte is able to parasitize pathogen hyphae, impairing their growth), and iii) substrate competition (the endophyte is able to grow more efficiently than the pathogen, without evidence of an inhibition zone).

Volatile antifungal assay

To test the emission of antifungal volatile organic compounds (VOCs) produced by the three fungal endophytes, a VOC assay was performed as described by Chen et al. (2018). Fungal endophytes were cultured independently in 3.5% YEA petri dishes and confronted "mouth-to-mouth" against *O. novo-ulmi*. In the case of P5 and YM11, the culture comprised 10 mg ml^{-1} of yeast cells or mycelial fragments. YCB36 was subcultured directly from the colony edge. The two plates (endophyte vs *O. novo-ulmi* and control with no endophyte vs *O. novo-ulmi*) were sealed together with parafilm and incubated vertically at 22 ^{o}C. Three replicates were performed for each endophyte. *O. novo-ulmi* mycelial growth was evaluated at 3, 7 and 10 days by scanning the plates and measuring the colony area using ImageJ free software. Inhibition of *O. novo-ulmi* growth was quantified as described in the previous section.

Antibiotic effect of liquid filtrates against O. novo-ulmi

Endophyte antibiotic potential against *O. novo-ulmi* was evaluated by obtaining liquid filtrates from endophytes. The inoculum source for each liquid culture was obtained by growing each endophyte on 3.5% YEA medium over an autoclaved cellophane layer. Once grown, endophyte fresh mycelia or yeast cells were harvested, adjusted to 5 mg ml^{-1} with sterile deionized water, and homogenized using an all-glass tissue homogenizer. For each endophyte, 100 µl of the fungal biomass homogenate was added to 70 ml of yeast, malt and glucose liquid medium (4g l^{-1} yeast extract, 10 g l^{-1} malt extract and 4 g l^{-1} glucose; YMG) in Erlenmeyer flasks and grown in the dark at 22 ^{o}C in an orbital shaker (120 rpm). Three replicates were performed for each fungal strain. Glucose content in the liquid media was quantified periodically by the anthrone-sulphuric acid quantification method (Laurentin and Edwards, 2003) using 96-well microplates. The values were quantified according to a standard curve with known concentrations of glucose (0-1000 ppm). Once glucose was totally consumed (at around 25 days of growth), the culture was left to grow for two more weeks to allow secretion of fungal metabolites. After this period, the broth culture was filtered, first with Whatman® filter paper grade 1 (Whatman International Ltd, Maidstone, UK) and subsequently with a sterile 0.2 µm PES syringe filter (Thermo Fisher

Scientific, Waltham, MA, USA), to separate broth and fungal biomass. The filtrates were preserved at 4 °C until use. The antibiotic effect of the liquid filtrates was assessed by growing *O. novo-ulmi* spores in their presence in microplates. To obtain O*. novo-ulmi* spores, mycelial fungal plugs were grown in Erlenmeyer flasks with Tchernoff's liquid medium (Tchernoff, 1965) at 22 °C in the dark, under constant shaking to induce sporulation. Three days later spores were collected by centrifugation and adjusted to 10^6 cells ml^{-1} using a haemocytometer. Six well-replicates were used for each treatment and control group. Microplates were incubated at 22 °C in the dark and growth was evaluated at 0, 2, 7, 9 and 11 days by reading the OD at 630 nm, using a spectrophotometer (ELx808, BioTek, Winooski, VE, USA) (Martín et al., 2010). To evaluate the effect of fungal filtrates, 100 µl filtrate was mixed with 100 µl *O. novo-ulmi* spores resuspended in *O. novo-ulmi* liquid filtrate, obtained following the same protocol as for the endophyte liquid filtrates (100 µl of 5 mg ml^{-1} homogenized fresh mycelia grown in YMG for 40 days). Pathogen growth in endophyte liquid filtrates (testing wells) was compared with growth in control wells containing 100 µl *O. novo-ulmi* spores resuspended in their own liquid filtrate, mixed with a further 100 µl *O. novo-ulmi* liquid filtrate. Additional background control wells containing endophyte or *O. novo-ulmi* filtrates only (without living cells) were used to subtract the optical density (OD) of the filtrates from the testing wells, thus measuring only the increased OD due to *O. novo-ulmi* growth. Background control wells also determined that culture filtrates contained no contamination. Comparison between treatment and control groups permitted calculation of *O. novo-ulmi* growth inhibition due to filtrates.

Proteolytic and chitinolytic activities

Extracellular protease and chitinase production by each fungus was evaluated in petri dishes with specific culture media at 5, 8, 12, 15, 20 and 23 days of incubation. Plugs of the fungal colonies were grown at 22 °C in the dark. Protease activity was determined on skim milk agar plates (SMA: 28 g l^{-1} skim milk powder, 5 g l^{-1} tryptone, 2.5 g l^{-1} yeast extract, 1 g l^{-1} glucose, 15 g l^{-1} agar; pH 7.0). Positive activity was measured by production of a clear halo surrounding the

colonies (Mayerhofer et al., 1973). The halo area (cm^2) was calculated by subtracting the colony area from the area inside the halo contour surrounding the colony. Chitinase detection medium was prepared as described by Agrawal and Kotasthane (2012). Colloidal chitin was obtained according to Castro et al. (2011). Bromocresol purple dye (Sigma-Aldrich, Darmstadt, Germany) permitted visualization of chitin degradation. A colour shift from yellow to purple around the colony indicates positive chitinase activity. The area showing a colour change was quantified (cm^2) by subtracting the colony area from the area of the colour-changed halo. Six replicates were performed for each fungus and activity.

Nutrient acquisition mechanisms

Siderophore and HCN production and phosphate solubilization potential were evaluated for each fungus at 5, 8, 12, 15, 20 and 23 days of incubation. Siderophore emission was examined using the Chrome Azurol S (CAS) agar medium. CAS was prepared following the protocol of Schwyn and Neilands (1987), in which 60.5 mg CAS (Merck KGaA, Darmstadt, Germany) was dissolved in dH_2O and mixed with 10 ml of iron (III) solution (1mM $FeCl_3.6H_20$, 10 mM HCl). After this, hexadecyltrimethylammonium bromide (HDTMA; Sigma-Aldrich, Darmstadt, Germany) was dissolved in water, mixed with CAS solution and autoclaved at 121 ^oC. The basal medium was prepared using 0.5 % succinic acid, 0.4 % KH_2PO_4, $(NH_4)_2SO_4$ and 2 % agar at pH 5.3. The HDTMA-CAS solution was slowly mixed until the desired blue colour was obtained. Plugs of fungal colonies were grown in six replicate petri dishes at 22 ^oC in the dark. Positive siderophore activity was evaluated by colour change from blue to yellow, subtracting the colony area from the area of the colour-changed halo (cm^2).

The hydrogen cyanide (HCN) production test was performed based on Millar and Higgins (1970). HCN solution was prepared by mixing 0.5% picric acid and 2% sodium carbonate. Sterilized Whatman® filter papers were soaked in HCN solution. Fungal plugs were cultured on 3.5% YEA and filter papers were placed on the lid of the petri dish, which was then closed and incubated

in the dark at 22 °C. Six replicates were performed for each fungus. Colour change in the filter paper indicates positive HCN release by the fungi, due to the ability of HCN to reduce picric acid to isopurpuric acid. Activity was scored as negative (no colour change) or positive (brown to reddish brown).

Phosphate solubilization was performed in Pikovskaya agar medium with the addition of 0.3 % insoluble calcium triphosphate (Sigma-Algrich, Darmstadt, Germany). Endophyte plugs were grown in six replicate petri dishes at 22 °C in the dark. The presence of a halo or clear area around the colony, indicating phosphate solubilization potential, was measured as halo area (cm^2).

Nutrient utilization patterns and chemical sensitivity

Nutrient utilization patterns and the sensitivity of the endophytes and the pathogen to a series of inhibitory substrates were evaluated using in-house configured phenotypic microarrays, following the methodology described by Blumenstein et al. (2015). Fungal inocula were prepared as described in the section "Antibiotic effect of liquid filtrates against *O. novo-ulmi*", but in this case the fungal biomass was resuspended in Murashige and Skoog (MS) liquid medium. Fungal growth on different nutrients was evaluated in 96-well microplates by measuring OD at 630 nm using an ELx808 spectrophotometer after 9 days of incubation. The following carbon sources were added individually to the MS medium: glucose, fructose, sucrose, cellobiose, pectin, xylose, maltose, starch and carboxymethyl-cellulose. All nutrient solutions were adjusted to a final concentration of 0.25 M carbon atoms. Various metabolites with potential to inhibit fungal development were added individually to the MS medium: gallic acid (1 g l^{-1}), salicylic acid (0.05 g l^{-1}), tannic acid (1 g l^{-1}), veratryl alcohol (2.37 g l^{-1}), quercetin (0.01 g l^{-1}), catechin (1 g l^{-1}), thymol (0.05 g l^{-1}) and ethanol (5%). Carbon consumption by endophytes was compared with carbon consumption by *O. novo-ulmi* using the Niche Overlap Index (NOI). NOI was calculated as the number of carbon sources consumed by the endophyte and the pathogen, divided by the number of sources consumed by the pathogen (Lee and Magan, 1999).

An NOI value of 0.9 or above indicates a high degree of niche overlap and a competitive disadvantage for the pathogen (Blumenstein et al., 2015).

Phytohormone production by endophytes and the pathogen

Ability to produce auxins and gibberellins was evaluated in the three endophytes and in *O. novo-ulmi*. For indole-3-acetic acid (IAA) detection, the four fungi were grown separately in 2% malt extract broth (MEB) containing 0.2% (v/v) L-tryptophan. Erlenmeyer flasks contained 30 ml medium and 60 µl homogenized fungal biomass adjusted to 5 mg ml^{1}. Flasks were kept in the dark at 22 ^{o}C under constant shaking for 15 days. IAA production was estimated following the colorimetric protocol, using Salkowski reagent described in Gang et al. (2019) prepared by mixing 0.5 M ferric chloride ($FeCl_3$) and 35% perchloric acid ($HClO_4$). Three replicates were performed for each fungus. To quantify the IAA produced by each fungus, three aliquots of each broth were selected and centrifuged at 10,000 rpm for 10 min. After that, 500 µl supernatant was mixed with 1 ml Salkowski reagent and incubated for 25 min in the dark. Absorbance was read at 530 nm, and the concentration of IAA produced by each isolate was determined using a standard curve of pure IAA (Sigma-Aldrich, Darmstadt, Germany) ranging from 0 to 1000 µg ml^{-1}.

Gibberellic acid (GA_3) released by each fungus was quantified using the liquid filtrates obtained for the antibiotic evaluation (see previous section). GA quantification was performed by selecting three aliquots of the filtrate and adjusting the pH to 1.5 using 0.1 M HCl. Then, 2 ml of the acidified liquid medium was mixed with 4 ml ethyl acetate, vortexed vigorously and centrifuged at 5,000 rpm for 10 min. This process was repeated two more times, after which the organic phase was mixed, evaporated and suspended in absolute ethanol. Absorbance was read at 254 nm and recorded at 20 s intervals for 2 min according to Berrios et al. (2004). GA_3 concentration was estimated using GA_3 (Sigma-Aldrich, Darmstadt, Germany) standard solutions in ethanol ranging from 0 g l^{-1} to 1 g l^{-1}.

In vivo experiment

Plant material

The plant material used in the *in vivo* experiment was produced in 2012 as part of the regular activities of the Spanish elm breeding programme at Puerta de Hierro Forest Breeding Centre. Controlled crosses were performed between two *U. minor* genotypes (M-CC1 and AL-AN1). To properly evaluate offspring susceptibility to DED, the seedlings obtained (N=37) were cloned through aerial cuttings. After the susceptibility tests, four seedlings showing moderate to high DED susceptibility (50-70 % leaf wilting 60 days after *O. novo-ulmi* inoculation) were selected and 30 to 34 clonal replicates of each seedling were planted in an experimental plot in 2014 (Table 1). The plot had a complete random design and plants were spaced 1 × 1.4 m apart. Plants were regularly watered in spring and summer to avoid water stress. One highly DED resistant commercial clone (Sapporo, N=8) and one highly DED susceptible clone (M-PZ3, N=8) were also included in the plot to confirm the virulence of the *O. novo-ulmi* isolate.

Experimental design

In planta inoculations were performed in May 2017, when plants were 6 years old. Two endophyte cell suspensions were prepared (as described in the next section): (i) a mixture of P5 and YM11; and ii) YCB36. These suspensions were inoculated into the vascular system in the middle of the trunk using an endotherapy device (BITE, Padova, Italy). *Ophiostoma novo-ulmi* inoculations were performed with a bud-cell suspension (prepared as described in the next section) 5 cm below the endophyte inoculation point, on the opposite side of the trunk. Pathogen spores were delivered into the xylem sap stream through a transverse cut made with a sharp blade (Solla et al., 2005). Four treatments were applied (Fig. S1): (i) Control plants with no endophyte or pathogen inoculation (E-O-); (ii) Plants inoculated with endophytes (P5+YM11 or YCB36) without subsequent *O. novo-ulmi* inoculation (E+O-); iii) Plants inoculated with *O. novo-ulmi* without previous conditioning endophyte inoculation (E-O+); and iv) Plants inoculated with endophytes subsequently inoculated with the pathogen (E+O+) (Table 1). In treatments i)

to iii), plants not inoculated with either the endophytes or the pathogen (E- and O- treatments) received sterile distilled water on 1 May (E-) and 16 May (O-), respectively.

Inoculum preparation

To obtain the endophyte inoculum, a liquid suspension of bud cells (for YM11 and P5) or hyphal fragments (for YCB36) were prepared. Endophytes were grown in petri dishes containing 3.5% YEA, with (for YM11 and YCB36) or without (for P5) an autoclaved cellophane layer, for 10 days at 22 ^{o}C in the dark. P5 yeast cells were scraped from the agar using a sterile spatula and suspended in sterile distilled water. YM11 formed a colony of dense, hard agglomerates of bud cells, requiring the use of an all-glass tissue homogenizer to obtain a homogeneous cell suspension. YCB36 did not produce sufficient quantity of conidia and therefore spores were replaced by mycelial fragments also obtained using an all-glass tissue homogenizer (obtaining fragments of four or fewer cells). Aqueous suspensions of yeast cells or mycelial fragments were adjusted using a haematocytometer to obtain a final inoculum concentration of 2 x 10^6 cells ml^{-1} for the mixture of P5 and YM11 (10^6 cells ml^{-1} of each fungus) and 10^6 cells ml^{-1} for YCB36.

To obtain O*. novo-ulmi* spores, mycelial fungal plugs were grown in Erlenmeyer flasks with Tchernoff's liquid medium (Tchernoff, 1965) at 22 ^{o}C in the dark under constant shaking to induce sporulation. Three days later, spores were collected by centrifugation and adjusted to 10^6 blastospores ml^{-1} using a haemocytometer.

Leaf wilting evaluation

Leaf yellowing and wilting are typical DED symptoms. As the disease progresses, a mixture of healthy and suffering foliage may be seen (Brasier and Buck, 2001) and the percentage of foliar wilting in the crown is a good indicator of tree decline (Solla et al., 2005). Leaf wilting was evaluated in each tree at 30, 60 and 120 days post inoculation (dpi) with *O. novo-ulmi* and also 1 year post-inoculation (ypi). Assessments were performed by three independent evaluators and the mean of the three scores was calculated for each tree and treatment. A representative

leaf of the average wilting status of the tree was selected to measure stomatal conductance. This measurement was made at the time of *O. novo-ulmi* inoculation and at 30 dpi using an SC-1 leaf porometer (Decagon Devices, Washington, USA) in five trees per treatment, at midday on both occasions.

In planta endophyte quantification

To evaluate plant colonization by endophytes, wood samples from control (E-O-) and endophyte-treated trees (E+O-) were extracted using an increment borer at 75 days and 1 year after endophyte inoculation. Two samples per tree were taken, at 5 and 50 cm above the endophyte inoculation point. Three replicate trees per treatment were evaluated. Fungal DNA presence was quantified through quantitative PCR (qPCR). First, core wood samples were ground to a fine powder in a ball mill (Mixer mill MM 400, Retsch GmbH, Haan, Germany) and DNA was extracted using the Norgen plant/fungi DNA isolation kit (Norgen Biotek Corp., Thorold, ON, Canada), obtaining high yield and quality scores. Primer sequences were designed within the sequences obtained by ITS Sanger sequencing of each fungus (described previously) using Primer3 Version 0.4.0 (http://bioinfo.ut.ee/primer3-0.4.0/primer3/) and following specific parameters for qPCR primer design (Udvardi et al., 2008). Specificity tests for the primers designed were performed by selecting 10 additional fungi available in our collection and amplifying fungal DNA through conventional PCR. If an amplification product was observed, the primer pair was discarded and new primer pairs were designed. Selected primer pairs were set as follows: the primer pair for P5 fungi (forward primer: 5'-CAACGGATCTCTTGGCTCTC-3'/ reverse primer: 5'-AACAGACATACTCTTCGGAATACC-3') created a 136 base-pair (bp) product, the primer pair for YM11 (forward primer: 5'- AGGAACTGGCCTCAAAGACA-3'/ reverse primer: 5'-TCCTACCTGATCCGAGGTCA -3') created a 142 bp product, and the primer pair for YCB36 (forward primer: 5'-AGTATACGCCGCCTTGACAC-3'/ reverse primer: 5'-GTCGTAAAACATGGGGAACG-3') created a 130 bp product. Fungal DNA quantifications were performed independently for each fungus using SSoFast EvaGreen® Supermix (Bio-Rad

Laboratories, Irivine, CA, USA) in a CFX96 real-time PCR detection system thermocycler (Bio-Rad Laboratories, Irvine, CA, USA). Fungal DNA was standardized per quantity of plant DNA by amplifying a fragment of the *U. minor* ITS region (ITSUlmi) (forward primer: 5'-ATATGTCAAAACGACTCTCGGCAAC-3'/ reverse primer: 5'-AACTTGCGTTCAAAGACTCGATGGT-3'). In triplicate, reactions contained 2 µl sample DNA and 8 µl master mix. Following a first denaturation step at 95 °C for 30 s, 40 cycles were performed at 95 °C for 5 s and 60 °C for 30 s. Each plate included two replicates of each sample: one for amplification of the specific fungal ITS, and the other for amplification of *U. minor* ITS. Three no-template controls were included for each primer pair. The amplification results were analysed and expressed as fungal abundance relative to non-inoculated plants.

Plant biochemical measurements

Wood samples were extracted from trees showing a significant effect of the endophyte conditioning treatment on plant symptomatology, to measure non-structural carbohydrates, total phenolic and flavonoid content, and proline. The concentration of non-structural carbohydrates (NSC) was measured using a modified protocol from Maness (2010). Soluble sugars (SS) were extracted by incubating 50 mg fresh material in 1 ml of 80% ethanol. An aliquot of the ethanol extract was reserved for proline quantification (see below). The insoluble material in the pellet was used for starch determination. Sugar monomers from the ethanol extract or starch digestion were quantified by the anthrone-sulphuric acid colorimetric microassay, based on Laurentin and Edwards (2003), using 96-well microplates. The values were quantified according to standard curves with known concentrations of glucose, fructose and galactose (0-1000 ppm) in the case of SS, and only glucose (0-1000 ppm) in the case of starch. Total NSC concentration was calculated by adding the concentrations of SS and starch.

Total phenolic content extraction was performed according to a microplate-adapted protocol described by Ainsworth and Gillespie (2007) and quantified using the Folin-Ciocalteu reagent (F-

C). Briefly, 20 mg powdered wood was extracted in 1 ml of 95 % methanol under constant shaking in a mixer mill (Precellys, Bertin Instruments, Montigny-le-Bretonneux, France), then incubated at room temperature for 48 h in the dark. The supernatant was recovered and 200 µl of the F-C reagent at 10% (v/v) was added per each 100 µl of extract or standard. Finally, 800 µl of Na_2CO_3 700 mM was added and incubated at room temperature for 2 h. Absorbance was read at 765 nm and the values were quantified according to a standard curve with known concentrations of gallic acid (25 µM-1.5 mM). Results were expressed as mg equivalent gallic acid per gram of fresh weight of sample.

Total flavonoid content was determined using the same extract obtained for total phenolic content and quantified by the colorimetric method described in Barreira et al. (2008), with slight modifications. Briefly, 177.5 µL aliquots of each sample and 25 µL aliquots of each standard point (diluted with 152.5 µL deionized water) were mixed with $NaNO_2$ (5%, 7.5 µL). After 6 min, 15 µL of a 10% $AlCl_3 \cdot 6H_2O$ solution was added, and after 5 min incubation at room temperature, 50 µL of 1M NaOH was added. The absorbance of each blank, consisting of the same sample mixtures but with deionized water instead of 10% $AlCl_3 \cdot 6H_2O$ solution, was subtracted from the test absorbance. The absorbance was read at 510 nm using a microplate reader and the values were quantified according to a standard curve with known concentrations of quercetin (0.2-1.0 mg ml^{-1} in ethanol). Results were expressed as mg equivalent quercetin per gram of fresh weight of sample.

Free proline content was determined with the same extract used for SS determination. Quantification was carried out using a microplate reader protocol (Carillo and Gibon, 2011). In each well, 50 µl of the ethanolic extract, blank or proline standards (1-0.4-0.2-0.1-0.04 mM) was mixed with 100 µl of the reaction mix: 1 % ninhydrin (w/v) in 60% acetic acid (v/v) and 20% ethanol (v/v). Plates were incubated in a water bath at 95 ^{o}C for 20 min and absorbance was

read at 520 nm. The readings were transformed to proline contents (nmol mg^{-1} FW) according to Carillo and Gibon (2011).

Statistical analysis

The effect of endophytes on *O. novo-ulmi* growth in *in vitro* assays was tested with one-way ANOVA and the post-hoc Fisher's Least Significant Difference (LSD) test ($P<0.05$). The area of the halo formed by the four fungal strains was compared using a one-way ANOVA test followed by Fisher's LSD test ($P<0.05$) to identify differences in protease, chitinase and siderophore emission between isolates. The effect of inhibitory substances and carbon sources on fungal growth was represented with a two-way joining cluster analysis using the heatmap function in the "pheatmap" package in R-studio (R Core Team 2017). Euclidean distances were used in the clustering of fungal endophytes or chemicals. Differences in wilting symptoms, leaf stomatal conductance and biochemical variables were analysed with one-way ANOVA test followed by Fisher's LSD test ($P<0.05$). To observe differences in wilting symptoms among elm clones due to *O. novo-ulmi*, a factorial ANOVA was performed, taking the clone and *O. novo-ulmi* treatments as factors. Fungal quantification through quantitative PCR was performed for each sample at 5 and 50 cm from the inoculation point with three technical replicates per PCR plate. The cycle threshold value (Ct) obtained for the plant and endophyte ITS in each sample was transformed to double delta Ct (ΔΔCt). Then, ΔΔCt of the endophyte was normalized to ΔΔCt of plant ITS. The normalized values of endophyte-treated plants were relativized to control plants, obtaining the fold-change of endophyte presence. These values were analysed with a one-way ANOVA test to determine whether there were significant differences between inoculated and non-inoculated trees.

Analyses were run using STATISTICA version 8.0 (StatSoft, Tulsa, OK, USA) and R software (R Core Team 2017). In all cases, normality was confirmed before ANOVA analysis with skewness and kurtosis values and the Kolmogorov-Smirnov test.

Results

Molecular identification of fungal endophytes

According to the ITS sequencing, the P5 endophyte was identical to Genebank sequence accessions LC493223.1 and LC493222.1 identified at genus level as *Cystobasidium* (Cystobasidiomycetes) (Table 2). The YM11 endophyte showed the highest similarity level (99%) with genus *Exophiala* (Eurotiomycetes). The YCB36 isolate was not identified at the genus level. The most similar hit (98 % of identity) indicates that this fungus probably belongs to the Dothideomycetes class, and according to the third hit it may be tentatively classified within the Phaeosphaeriaceae family.

In vitro fungal endophyte characterization

In vitro endophyte-pathogen interactions

O. novo-ulmi growth was reduced when confronted with YCB36 endophytes, but not with YM11 or P5 (Fig. 1a; Fig. S2). Growth reduction was higher at day 7 (37.62 ± 5.32 %) and decreased to 33.16 ± 4.03 % at day 10 and 28.05 ± 3.59 % at day 12 (Fig. 1a; Fig. S2). *O. novo-ulmi* growth was also inhibited by volatiles emitted by P5 and YCB36 endophytes. The highest inhibition was observed at day 10 of incubation with YCB36 (32.82 ± 5.54 %) (Fig. 1b; Fig. S2). P5 also caused moderate inhibition of *O. novo-ulmi* growth at day 10 (11.02 ± 3.28 %) (Fig. 1b; Fig. S2).

Antibiotic traits evaluation

O. novo-ulmi growth was reduced in the presence of YM11 and YCB36 liquid filtrates (Fig. 1c). YCB36 filtrate was able to reduce *O. novo-ulmi* growth from day 4 onwards (Fig. 1c), with a peak in inhibition at day 9 (55.94 ± 0.96 % growth reduction; $P<0.01$). YM11 filtrate also caused the highest inhibition of *O. novo-ulmi* growth at day 9 (28.74 ± 2.9 % growth reduction). P5 filtrate did not reduce *O. novo-ulmi* growth. Proteolytic activity varied considerably among isolates, with *O. novo-ulmi* showing the largest halo formation at day 20 (28.73 cm^2; Table 3, Fig. S2). Endophyte P5 showed low proteolytic activity, which was barely visible at days 10 and 14 (0.59

± 0.51 and 1.33 ± 0.07 cm^2). In contrast, YCB36 and YM11 showed a clear halo around the colony from day 8 (Fig. S2). At day 20, proteolytic activity was significantly higher for YCB36 than for YM11 (10.28 ± 2.48 and 5.75 ± 0.71 cm^2, respectively) (Table 3). In the case of chitinolytic activity, YCB36 produced a clear blue-purple halo surrounding the colony (18.19 cm^2 at day 5 and 49.85 ± 1.63 cm^2 at day 20), while the other endophytic fungi showed no chitin degradation ability (Table 3, Fig. S2). Chitinase activity in *O. novo-ulmi* became visible at day 20 (6.46 ± 1.96 cm^2) (Table 3, Fig. S2).

Nutrient acquisition mechanisms and nutritional niche

Only the *O. novo-ulmi* and YCB36 isolates showed positive siderophore emission into the medium (Table 3, Fig. S2). YCB36 exhibited greater halo formation than *O. novo-ulmi* at day 20 (7.90 ± 0.44 vs 5.39 ± 0.98 cm^2) ($P<0.05$) (Table 3, Fig. S2). However, neither HCN nor phosphate solubilization activities were positive in any of the fungal strains evaluated (Table 3).

The carbon utilization pattern and chemical sensitivity to inhibitory substances of each isolate are shown in the two-way joining cluster graph (Fig. 2). As expected, the analysis of the substrates (vertical axis) provided two clusters: the carbon sources on one side and the inhibitory metabolites on the other. The clustering of the fungal isolates (horizontal axis) separated P5 from the other fungi, coinciding with the taxonomic division of the fungi into Basidiomycota and Ascomycota, respectively. The clustering also separated the two ascomycetous endophytes (YM11 and YCB36) from the pathogen. P5 and *O. novo-ulmi* were less affected by inhibitory metabolites (e.g., by gallic acid and thymol), while YM11 and *O. novo-ulmi* showed the highest growth in the presence of certain carbon sources (e.g., sucrose, glucose and fructose).

Considering carbon sources only, the NOI of *O. novo-ulmi* with regard to P5, YM11 and YCB36 was 0.78, 0.78 and 1, respectively, indicating a putative high niche overlap between the pathogen and YCB36.

Growth promotion potential

The three endophytes and the pathogen produced IAA. *O. novo-ulmi* produced 191.23 µg g^{-1} IAA per fungal dry weight. P5 produced 1110.14 µg g^{-1} fungal dry weight and was the endophyte with highest IAA production (Fig. 3a). GA_3 production was similar in *O. novo-ulmi*, YCB36 and P5 (3.93 ± 0.30, 5.16 ± 0.19 and 3.46 ± 0.41, respectively), while YM11 displayed the lowest GA_3 production (1.64 ± 0.08) (Fig. 3b).

In vivo assay

Leaf wilting evaluation and stomatal conductance

Leaf wilting at 120 dpi in the resistant control clone Sapporo was low (5.94 % ± 2.59; mean ± SE) but high in the susceptible control clone M-PZ3 (68.33 % ± 11.76), confirming the virulence of the *O. novo-ulmi* isolate inoculated. Trees that were not inoculated with *O. novo-ulmi* (E-O- and E+O-) showed no leaf yellowing or wilting symptoms, while trees inoculated with the pathogen (E-O+ and E+O+) displayed various levels of leaf wilting. The four genotypes of the progeny (M-CC1 × AL-AN1) exhibited a similar response to *O. novo-ulmi* (P = 0.423). Therefore, the effect of the genotype was not considered in subsequent analyses. Trees without conditioning inoculation with endophytes (E-O+) showed mean leaf wilting values of 48.93 to 66.95% at different evaluation dates (Fig. 4a,c). Trees conditioned with P5+YM11 before *O. novo-ulmi* inoculation (E+O+) showed similar symptoms to non-conditioned trees (E-O+) (Fig. 4a). In this case, the proportion of trees with leaf wilting percentages higher than 50% was similar in E-O+ and E+O+ plants at 120 dpi (Fig. 4b). However, trees conditioned with YCB36 (E+O+) showed lower wilting symptoms than non-conditioned trees (E-O+) at 30, 60 and 120 dpi (Fig. 4c). In this case, the proportion of trees with leaf wilting percentages higher than 50% was lower in E+O+ trees than in E-O+ trees at 120 dpi (Fig. 4d). After 1 year, however, the protective effect of the YCB36 isolate was no longer evident (Fig. 4c).

In addition, *O. novo-ulmi* inoculation caused a decline in stomatal conductance at 30 dpi, both in trees pre-conditioned with P5+YM11 (E+O+) (Fig. 5a,b) and E-O+ trees (Fig. 5a,b). YCB36-treated trees (E+O-, Fig 5b) showed higher stomatal conductance at 30 dpi than non-treated trees (E-O-, Fig. 5b).

In planta endophyte quantification

At 75 dpi, P5 presence near the inoculation point was 4.81 times higher than in non-inoculated trees ($P<0.05$). At 50 cm, however, no significant differences were observed ($P>0.05$). The presence of YM11 in inoculated trees was 9.09 times higher than in non-inoculated trees at 50 cm from the inoculation point ($P<0.05$) (Fig. 6a). YCB36 showed increased presence at both 5 and 50 cm above the inoculation point (4.64 and 17.86 times) ($P<0.05$) (Fig. 6a). In all cases, amplification of ITS sequences in non-endophyte inoculated trees occurred in later cycles for YCB36 than for YM11 and P5, indicating a higher basal presence of P5 and YM11 than YCB36 in non-endophyte-treated elms.

One year after inoculation, endophyte presence was typically lower than in 75 dpi quantifications (Fig. 6b). P5 and YCB36 presence was still higher than in control plants at 50 and 5 cm from the inoculation point, respectively. Conversely, the presence of YM1 to basal levels, showing no statistically significant differences with non-inoculated trees ($P>0.05$).

Biochemical changes induced in endophyte-treated trees

Potential mechanisms of induced resistance were explored in YCB36-treated plants, as this was the only treatment that showed a protective effect against *O. novo-ulmi* in the trees. Soluble sugars and starch content were not modified by endophyte inoculation ($P>0.15$). However, both flavonoids and total phenols were significantly modified by YCB36 treatment. Flavonoid content was higher in YCB36-treated trees than in controls at 50 cm from the inoculation point ($P<0.05$). Total phenols increased at both 5 and 50 cm from the inoculation point ($P<0.05$) (Fig. 7a,b).

Proline content significantly decreased in endophyte-treated trees at 50 cm above the inoculation point (Fig. 7c).

Discussion

This work explores the functional ecology of tree fungal endophytes and the mechanisms through which they could potentially improve resistance to a fungal pathogen. According to the phenotypic traits of the endophytes, P5 (*Cystobasidium*) can be classified within the group of plant growth-promoting pink yeasts (Joubert and Doty, 2018) and YM11 (*Exophiala*) within the dark septate endophytes (DSE) (Andrade-Linares and Franken, 2013), also known as black yeasts (Sudhadham et al., 2008). Several endophytic yeasts in these groups stimulate plant growth, increase yield or reduce biotic or abiotic damage (Punja and Utkhede, 2003; El-Tarabily, 2004; Kandel et al., 2017; de Tenorio et al., 2019). Plant experiments performed with the pink yeast *Rhodotorula* spp. demonstrated increased phytoremediation ability (Silambarasan et al., 2019), strong inhibition of plant fungal or bacterial pathogens (Kalogiannis et al., 2006; Akhtyamova and Sattarova, 2013), increased plant germination rates (Akhtyamova and Sattarova, 2013) and increased root and shoot growth rates, mainly through their ability to synthesize phytohormones (Nutaratat et al., 2014; Sen et al., 2019). Moreover, DSE comprise a polyphyletic group of non-mycorrhizal ascomycetous fungi with potentially beneficial functions for their host plants, primarily in reducing biotic and abiotic stresses (Jumpponen and Trappe, 1998; Andrade-Linares, 2011). Plant studies on *Exophiala* spp. revealed their ability to increase host tolerance to abiotic stress by activating antioxidant enzymes (Khan et al., 2012) and improving plant growth through production of biologically active GAs (Khan et al., 2009). In our work, however, the *Exophiala* isolate (YM11) did not produce significant amounts of phytohormones and was the endophyte with lowest GA_3 production, while P5 showed high production of IAA in the *in vitro* experiment (Fig. 3a). These results raise doubts about the role of YM11 as a producer of plant growth hormones and support the classification of P5 within the plant growth-promoting pink yeasts group (Xin et al., 2009; Joubert and Doty, 2018). GA_3 and IAA are the main hormones

inducing cell proliferation and elongation, leading to enhanced root growth and stem elongation. Maintenance of high growth rates during *O. novo-ulmi* infection has been reported in small saplings as a resistance mechanism against the pathogen (Martín et al. 2019), and this mechanism could be enhanced in plants extensively colonized by hormone-producing yeasts. Although in the field assay the P5+YM11 treatment did not enhance tree resistance to DED, ongoing work with *in vitro* elm plantlets inoculated with a similar P5+YM11 inoculum revealed that this treatment induces higher root elongation and improves plant survival against drought (Martínez-Arias et al., unpublished results).

The dothideomycetous YCB36 isolate demonstrated strong *in vitro* antibiotic activity against *O. novo-ulmi.* We were unable to determine the identity of this fungus at the genus level using the ITS sequence, and it is likely an undescribed species. The most similar hits to YCB36 (see NCBI accession numbers, table 2) were also found to be associated endophytically with a *Quercus* species (Moricca et al., 2012; Doust et al., 2017). The activity of YCB36 against *O. novo-ulmi* in the *in vitro* dual culture assay evidenced strong pathogen inhibition without physical contact between mycelia (Fig. 1a; Fig. S2). YCB36 liquid exudates (evaluated in the antibiosis test) exerted the highest inhibition of *O. novo-ulmi*, supporting the previous results and suggesting release of antibiotic metabolites into the culture medium (Fig. 1c). The high hydrolytic activity of this endophyte may be involved in *O. novo-ulmi* growth inhibition. Both chitinolytic and proteolytic activities were highly positive in YCB36 (Table 3; Fig. S2), indicating that this fungus may have released these enzymes into the culture medium. Chitin is the major structural component of hyphal cell walls, and its enzymatic degradation via chitinases can disrupt or collapse fungal hyphae or even cause fungal death (Huang et al., 2007; Gruber and Seidl-Seiboth, 2012). For this reason, chitinolytic microorganisms have a potential application as biological control agents, as is the case of *Trichoderma harzianum* and *Beauveria bassiana* (Gruber and Seidl-Seiboth, 2012; Paredes et al., 2016). In turn, proteases are usually needed to facilitate fungal entry into host tissues, and also play an important role in pathogen virulence during the

entire infection cycle (Hueck, 1998; Figaj et al., 2019). In this experiment, as expected, the highest proteolytic activity was observed in *O. novo-ulmi*. This feature may give the pathogen an advantage over other fungi by enabling it to rapidly colonize elm xylem tissue. YCB36 also showed positive protease activity that could facilitate plant colonization and also affect *O. novo-ulmi* growth (Zhang et al., 2012).

Emission of antimicrobial VOCs by YCB36 may be another reason for the reduction in *O. novo-ulmi* growth. Several endophytic fungi have been reported to emit VOCs to establish a communicative interaction with their surroundings (Farre-Armengol et al., 2016; Roy and Banerjee, 2019). These molecules could have a potential role against fungal diseases due to their antimicrobial effects (Ezra et al., 2004; Chen et al., 2018; Wonglom et al., 2020) and ability to induce expression of defence genes in plants (Malmierca et al., 2012; Naznin et al., 2014; Pieterse et al., 2014). YCB36 showed the ability to reduce *O. novo-ulmi* growth when grown in confronted plates, probably through emission of volatile antibiotic molecules commonly attributed to terpenes, alcohols and carboxylic acids (Zhang et al., 2014). Both chitinase and VOC emission by YCB36 could also have a negative influence on *O. novo-ulmi* development in plant tissues and may have contributed to the reduced DED symptoms observed in YCB36-treated trees. Furthermore, a high nutritional niche overlap was observed between *O. novo-ulmi* and YCB36 in the nutrient utilization assay. Contrary to the results obtained by Blumenstein et al. (2015) with other elm endophytes, *O. novo-ulmi* and YCB36 showed the same range of metabolized carbon substrates, indicating a high nutritional niche overlap that could result in competitive interaction between endophyte and pathogen *in planta*. However, unlike YCB36, *O. novo-ulmi* is able to grow in the presence of certain inhibitory substances such as gallic acid and thymol, which could reflect its greater ability to cope with plant defensive metabolites.

Additionally, both *O. novo-ulmi* and YCB36 (in particular) displayed the ability to produce siderophores. Microorganisms use siderophores to obtain iron from the environment. In

pathogenic interactions, they enable iron acquisition from host proteins and have an essential role in virulence in several plant pathogens (Oide et al., 2006; Chen et al., 2013; Albarouki et al., 2014). In mutualistic symbiotic relationships between plants and fungi, siderophores produced by the fungal symbiont facilitate plant access to natural insoluble iron found in soil, improving plant growth (Kumar et al., 2018; Grobelak and Hiller, 2017). Many studies have also described the role of siderophores as stimulators of plant immunity (Buysens et al., 1996), in particular as activators of induced systemic resistance (ISR) (Beneduzi et al., 2012; Aznar and Dellagi, 2015), because they can be recognized as microbe-associated molecular patterns (MAMPs). Microbial gene-knockout on siderophore emission revealed the importance of these molecules for ISR elicitation (De Vleesschauwer et al., 2008).

In the *in vivo* experiment, endophyte inoculations were performed for the first time on elm trees using the BITE® endotherapy device. Fungal DNA amplification on E+O- wood samples confirmed the success of the inoculation system, with inoculated trees showing higher P5, YM11 or YCB36 fungal presence than non-inoculated trees (Fig. 6a,b). Nevertheless, the increased presence of these endophytes led to reduced symptoms after *O. novo-ulmi* inoculation only in YCB36-treated trees (Fig. 4c). YCB36 showed a higher plant colonization rate than P5 and YM11 (Fig. 6a,b), possibly enhanced by its high protease activity. In the long term (one year after inoculation), however, the presence of YCB36 in plant tissue was markedly reduced, and the YCB36 isolate no longer exerted a protective effect (Fig. 6d), similar to what occurs in preventive inoculations with *Verticillium albo-atrum* (Postma and Goossen-van de Geijn, 2016). In our case, despite the use of local elm endophytes, the elm fungal endobiome was resilient enough to reduce the presence of the artificially inoculated endophytes. This corroborates the assumption that the microbiome tends to be resistant and resilient to disturbances in community structure and has a composition that is very difficult to alter (Toju et al., 2018). The strength of microbiome communities seems to arise from pioneer colonizing fungi at early plant developmental stages, when they are able to use space and resources and limit or slow down the establishment of later colonizers (Wei et

al., 2015; Fukami et al., 2015). Therefore, managing the microbiome at early developmental stages using the targeted endophytes as early colonizers may be a worthwhile strategy for future experiments.

Interestingly, YCB36-treated trees (E+O-) showed increased stomatal conductance (Fig. 5b), suggesting that this endophyte has the ability to modulate plant physiological functions. Several studies have highlighted the considerable influence of microbial symbionts in host water relations (Rho and Kim, 2017, and references therein). Stomatal conductance is positively related to photosynthetic CO_2 uptake and, consequently, primary metabolism, which is involved in plant fitness and defence capability (Rosa et al., 2009). In this assay, no significant modifications in non-structural carbohydrates were observed, although we noticed a higher level of secondary metabolites (flavonoids and total phenolic content) in YCB36-treated trees than in untreated trees (Fig. 7c,d). Phenolic compounds are widely distributed in plants and play key roles in metabolic and physiological processes (Boudet, 2007; Kumar et al., 2018). These molecules also have antioxidant properties (Huang et al., 2007) that can ameliorate plant performance under stress conditions (Daayf et al., 2012; Cheynier et al., 2013; Mishra et al., 2018). Several studies have demonstrated increased synthesis of flavonoids and phenols in plants colonized by symbiotic microorganisms (Qawasmeh et al., 2012; Dupont et al., 2015). White et al. (2010) defended the hypothesis that enhanced production of antioxidants in endophyte-inoculated plants may be due to the plant response to endophyte-produced reactive oxygen species (ROS). Increased phenolic metabolites can also contribute to enhanced tree resistance to *O. novo-ulmi* in YCB36-treated trees, as reported in other elm studies (Witzell and Martín, 2008; Li et al., 2016). Moreover, accumulation of phenolic compounds may be linked to ISR activation. As described earlier, elm defence response could be triggered by YCB36 MAMPs, such as siderophores and VOCs. ISR activation is often regulated by a jasmonic/ethylene-dependent signalling pathway, and culminates with synthesis of pathogenesis-related proteins (PR proteins), synthesis of phytoalexins or, as observed in the YCB36-treated plants,

accumulation of phenolic compounds (Conrath at al., 2002). Proline content reduction in YCB36-inoculated trees may also indicate enhanced tree resistance. Lower proline levels have been described in various beneficial plant-microbe interactions, sometimes associated with better nutritional status and fitness and lower stress levels (Verslues and Sharma, 2010).

Three different mechanisms may have contributed to the reduction in DED symptomatology in YCB36-treated trees: i) induction of plant resistance mechanisms that indirectly inhibit *O. novo-ulmi* development (ISR activation and phenolic accumulation); ii) *O. novo-ulmi* niche displacement by YCB36 due to nutritional overlap; and iii) direct inhibition of *O. novo-ulmi* by YCB36 through chitinase, antifungal metabolites in liquid phase, and VOC emissions. These mechanisms could act independently or in combination. Examples include the symbiotic bacteria *Pseudomonas aeruginosa*, which is able to trigger ISR either through siderophore (Audenaert et al., 2002) or volatile emission (Ryu et al., 2004), and *Trichoderma* biocontrol fungi, which have been shown to activate defence genes through VOC emission and inhibit pathogen growth by interacting with hydrolytic enzymes (Malmierca et al., 2012).

Conclusions

Our study provides new evidence of the role of fungal endophytes in improving tree resistance to pathogens and the mechanisms underlying this activity. YCB36, the endophytic fungus with highest antibiotic activity in the *in vitro* test, significantly reduced DED symptomatology in the field test. Neither *Cystobasidium* sp. (P5) nor *Exophiala* sp. (YM11) isolates showed any effect on wilting symptoms. Despite this, both endophytic yeasts were successfully established on elm stems after artificial inoculation in adult trees, but in lower proportions than YCB36. Further studies are needed to determine the functional roles of these yeasts and their potential association with stress tolerance, and improve future field applications of YCB36 in elm trees. Because we observed a reduced YCB36 load one year after its application, annual or more frequent applications of the target endophyte are necessary. Additionally, more efficient

protocols, including different inoculum densities and other inoculation methods, need to be examined to optimize treatments. Other elm clones and environmental conditions should be tested to validate the results, because previous research demonstrated the significance of these variables in the results obtained (Martín et al., 2015). Also, high-throughput methods for conidia production need to be examined to obtain mass quantities of cells, as conidia are the most resilient and suitable cell type used in formulations for biocontrol treatments (Mancera-López et al., 2018). Future experiments must be specifically planned to enhance future large-scale application strategies.

Acknowledgments

We thank Jorge Dominguez, David Medel and David Macaya for assistance in plant propagation and endophyte isolation. This study was funded by the project GENESIS (AGL-2015-66952-R; MINECO/ERDF) and by an agreement for elm conservation between Universidad Politécnica de Madrid and *Dirección General de Desarrollo Rural y Política Forestal* (MAPA/EAFRD). C.M-A was supported by an FPI pre-doctoral fellowship from the Spanish Ministry of Economy and Competitiveness.

Supplementary material:

Fig. S1: Experimental procedure description. First, a cell fungal suspension was inoculated into the vascular system at the trunk base using an endotherapy device. *O. novo-ulmi* inoculations were performed 15 days later using a spore suspension, following traditional DED-inoculation methods. Four treatments were obtained for each endophyte combination (P5+YM11 or YCB36): E+ O-: endophyte-treated plants without *O. novo-ulmi* treatment; E- O+: *O. novo-ulmi*-treated plants without endophyte treatment; E+ O+: endophyte- and *O. novo-ulmi*-treated plants; and E- O-: non-inoculated plants (no endophyte or *O. novo*-ulmi inoculation). Leaf wilting was evaluated in each tree at 30, 60 and 120 days post (pathogen) inoculation (dpi) and 1 year post-inoculation (ypi) by three independent assessors. At 75 dpi a wood sample was cored with an increment borer (N=3) at 5 and 50 cm above the inoculation point for biochemical and fungal quantification measures. SS = soluble sugars.

Fig. S2: Fungal activities and *O. novo-ulmi* inhibition *in vitro* assay. Upper panel: protease, chitinase and siderophore *in vitro* activities performed by fungal endophytes and pathogen at day 20. Dotted red line delimits colony diameter; dotted yellow line delimits clear halo diameter. Chitinase and siderophore activity was negative (NA) for endophytes P5 and YM11. Lower panel: dual culture and VOC assay results. In the dual culture, *O. novo-ulmi* (white colony on left side

of the plate) is confronted against fungal endophytes (YCB36, P5 and YM11) (right side of the plate) at day 12. The VOC assay shows the results of *O. novo-ulmi* growth in the presence of endophytes at day 10. The scale bar below each petri dish indicates 1 cm length.

References

Agrawal T, Kotasthane AS. 2012. Chitinolytic assay of indigenous *Trichoderma* isolates collected from different geographical locations of Chhattisgarh in Central India. *SpringerPlus* **1 (1)**: 73.

Ainsworth EA, Gillespie KM. 2007. Estimation of total phenolic content and other oxidation substrates in plant tissues using Folin-Ciocalteu reagent. *Nature Protocols* **2**(4): 875-877.

Akhtyamova N, Sattarova RK. 2013. Endophytic yeast *Rhodotorula rubra* Strain TG-1: Antagonistic and plant protection activities. *Biochemistry and Physiology* 2:104. doi:10.4172/2168-9652.1000104

Albarouki E, Schafferer L, Ye F, von Wiren N, Haas H, Deising HB. 2014. Biotrophy-specific downregulation of siderophore biosynthesis in *Colletotrichum graminicola* is required for modulation of immune responses of maize. *Molecular Microbiology* **92**(2): 338-355.

Almario J, Jeena G, Wunder J, Langen G, Zuccaro A, Coupland G, Bucher M. 2017. Root-associated fungal microbiota of nonmycorrhizal *Arabis alpina* and its contribution to plant phosphorus nutrition. *Proceedings of the National Academy of Sciences of the United States of America* **114**(44): E9403-E9412.

Andrade-Linares DR, Franken P. 2013. Fungal Endophytes in plant roots: Taxonomy, colonization patterns, and functions. *Symbiotic Endophytes* **37**: 311-334.

Andrade-Linares DR, Grosch R, Restrepo S, Krumbein A, Franken P. 2011. Effects of dark septate endophytes on tomato plant performance. *Mycorrhiza* **21**(5): 413-422.

Arnold AE, Mejia LC, Kyllo D, Rojas EI, Maynard Z, Robbins N, Herre EA. 2003. Fungal endophytes limit pathogen damage in a tropical tree. *Proceedings of the National Academy of Sciences of the United States of America* **100**(26): 15649-15654.

Audenaert K, Pattery T, Cornelis P, Hofte M. 2002. Induction of systemic resistance to *Botrytis*

cinerea in tomato by *Pseudomonas aeruginosa* 7NSK2: role of salicylic acid, pyochelin, and pyocyanin. *Mol Plant Microbe Interact* **15**(11): 1147-1156.

Aznar A, Dellagi A. 2015. New insights into the role of siderophores as triggers of plant immunity: what can we learn from animals? *Journal of Experimental Botany* **66**(11): 3001-3010.

Barreira JCM, Ferreira ICFR, Oliveira MBPP, Pereira JA. 2008. Antioxidant activities of the extracts from chestnut flower, leaf, skins and fruit. *Food Chemistry* **107**(3): 1106-1113.

Bartholdy BA, Berreck M, Haselwandter K. 2001. Hydroxamate siderophore synthesis by *Phialocephala fortinii*, a typical dark septate fungal root endophyte. *Biometals* **14**(1): 33-42.

Beneduzi A, Ambrosini A, Passaglia LMP. 2012. Plant growth-promoting rhizobacteria (PGPR): Their potential as antagonists and biocontrol agents. *Genetics and Molecular Biology* **35**(4): 1044-1051.

Berrios J, Illanes A, Aroca G. 2004. Spectrophotometric method for determining gibberellic acid in fermentation broths. *Biotechnology Letters* **26**(1): 67-70.

Blumenstein K, Albrectsen BR, Martín JA, Hultberg M, Sieber TN, Helander M, Witzell J. 2015. Nutritional niche overlap potentiates the use of endophytes in biocontrol of a tree disease. *Biocontrol* **60**(5): 655-667.

Boudet AM. 2007. Evolution and current status of research in phenolic compounds. *Phytochemistry* **68**(22-24): 2722-2735.

Brasier CM, Buck KW. 2001. Rapid evolutionary changes in a globally invading fungal pathogen (Dutch Elm Disease). *Biological Invasions* **3**(3): 223-233.

Brasier CM, Lea J, Rawlings MK. 1981. The aggressive and non-aggressive strains of *Ceratocystis ulmi* have different temperature optima for growth. *Transactions of the British Mycological Society* **76**(2): 213-218.

Brenner K, You LC, Arnold FH. 2008. Engineering microbial consortia: a new frontier in synthetic

biology. *Trends in Biotechnology* **26**(9): 483-489.

dos Reis Almeida BF, Cerqueira FM, Silva RdN, Ulhoa CJ, Lima AL. 2007. Mycoparasitism studies of *Trichoderma harzianum* strains against *Rhizoctonia solani:* Evaluation of coiling and hydrolytic enzyme production. *Biotechnology Letters* **29**(8): 1189-1193.

Buysens S, Heungens K, Poppe J, Hofte M. 1996. Involvement of pyochelin and pyoverdin in suppression of Pythium-induced damping-off of tomato by *Pseudomonas aeruginosa* 7NSK2. *Appl Environ Microbiol* **62**(3): 865-871.

Carillo P, Gibon Y. 2011. PROTOCOL: Extraction and determination of proline. PrometheusWiki. http://www.researchgate.net/publication/211353600_PROTOCOL_Extraction_and_determination_of_proline

Carroll G. 1988. Fungal endophytes in stems and leaves - from latent pathogen to mutualistic symbiont. *Ecology* **69**(1): 2-9.

Castro R, Álvarez A, Machado E, Mendoza M, Gómez R, García P. 2011. Characterization of a extracellular chitinase produced by *Serratia* sp. BIOMI-363706 using colloidal chitin as substrate. *Revista de la Sociedad Química del Perú* **77**(2): 101-108.

Chamberlain K, Crawford DL. 1999. *In vitro* and *in vivo* antagonism of pathogenic turf grass fungi by *Streptomyces hygroscopicus* strains YCED9 and WYE53. *Journal of Industrial Microbiology and Biotechnology* **23**(1): 641-646.

Chen LH, Lin CH, Chung KR. 2013. A nonribosomal peptide synthetase mediates siderophore production and virulence in the citrus fungal pathogen *Alternaria alternata*. *Molecular Plant Pathology* **14**(5): 497-505.

Chen PH, Chen RY, Chou JY. 2018. Screening and evaluation of yeast antagonists for biological control of *Botrytis cinerea* on strawberry fruits. *Mycobiology* **46**(1): 33-46.

Cheynier V, Comte G, Davies KM, Lattanzio V, Martens S. 2013. Plant phenolics: Recent advances on their biosynthesis, genetics, and ecophysiology. *Plant Physiology and Biochemistry* **72**: 1-20.

Conrath U, Pieterse C, Mauch-Mani B. 2002. Priming in plant-pathogen interactions. *Trends in Plant Science* **7**(5): 210-216.

Daayf F, El Hadrami A, El-Bebany AE, Henriquez MA, Yao Z, Derksen H, El-Hadrami I, Adam LR. 2012. Phenolic compounds in plant defense and pathogen counter-defense mechanisms. In: Cheynier V, Sarni-Manchado P, Quideau S (eds). *Recent Advances in Polyphenol Research.* John Wiley & Sons, Ltd. Chichester, Uk. pp. 191-208.

Dastogeer KMG, Li H, Sivasithamparam K, Jones MGK, Wylie SJ. 2018. Fungal endophytes and a virus confer drought tolerance to *Nicotiana benthamiana* plants through modulating osmolytes, antioxidant enzymes and expression of host drought responsive genes. *Environmental and Experimental Botany* **149**: 95-108.

de Tenorio DA, de Medeiros EV, Lima CS, da Silva JM, de Barros JA, Neves RP, Laranjeira D. 2019. Biological control of *Rhizoctonia solani* in cowpea plants using yeast. *Tropical Plant Pathology* **44**(2): 113-119.

De Vleesschauwer D, Djavaheri M, Bakker PAHM, Hoefte M. 2008. *Pseudomonas fluorescens* WCS374r-Induced Systemic Resistance in Rice against *Magnaporthe oryzae* Is Based on Pseudobactin-Mediated Priming for a Salicylic Acid-Repressible Multifaceted Defense Response. *Plant Physiology* **148**(4): 1996-2012.

Doty SL. 2013. Endophytic yeasts: Biology and applications. *Symbiotic Endophytes* **37**: 335-343.

Doust NH, Akbarinia M, Safaie N, Yousefzadeh H, Balint M. 2017. Community analysis of Persian oak fungal microbiome under dust storm conditions. *Fungal Ecology* **29**: 1-9.

Dupont P-Y, Eaton CJ, Wargent JJ, Fechtner S, Solomon P, Schmid J, Day RC, Scott B, Cox MP. 2015. Fungal endophyte infection of ryegrass reprograms host metabolism and alters development. *New Phytologist* **208**(4): 1227-1240.

El-Tarabily KA. 2004. Suppression of *Rhizoctonia solani* diseases of sugar beet by antagonistic and plant growth-promoting yeasts. *Journal of Applied Microbiology* **96**(1): 69-75.

Ezra D, Hess WM, Strobel GA. 2004. New endophytic isolates of *Muscodor albus*, a volatile-

antibiotic-producing fungus. *Microbiology-Sgm* **150**: 4023-4031.

Fakhro A, Andrade-Linares DR, von Bargen S, Bandte M, Buettner C, Grosch R, Schwarz D, Franken P. 2010. Impact of *Piriformospora indica* on tomato growth and on interaction with fungal and viral pathogens. *Mycorrhiza* **20**(3): 191-200.

Farre-Armengol G, Filella I, Llusia J, Penuelas J. 2016. Bidirectional Interaction between Phyllospheric Microbiotas and Plant Volatile Emissions. *Trends in Plant Science* **21**(10): 854-860.

Fesel PH, Zuccaro A. 2016. Dissecting endophytic lifestyle along the parasitism/mutualism continuum in Arabidopsis. *Current Opinion in Microbiology* **32**: 103-112.

Figaj D, Ambroziak P, Przepiora T, Skorko-Glonek J. 2019. The role of proteases in the virulence of plant pathogenic acteria. *International Journal of Molecular Sciences* **20**(3).

Fukami T. 2015. Historical contingency in community assembly: Integrating niches, species pools, and priority Effects. *Annual Review of Ecology, Evolution, and Systematics.* **46**: 1-23.

Gang S, Sharma S, Saraf M, Buck M, Schumacher J. 2019. Analysis of Indole-3-acetic Acid (IAA) Production in Klebsiella by LC-MS/MS and the Salkowski Method. *Bio-Protocol* **9**(9).

Gao FK, Dai CC, Liu X. 2010. Mechanisms of fungal endophytes in plant protection against pathogens. *African Journal of Microbiology Research* **4**(13): 1346-1351.

Gibb EA, Hausner G. 2005. Optional mitochondrial introns and evidence for a homing-endonuclease gene in the mtDNA rnl gene in *Ophiostoma ulmi* s. lat. *Mycological Research* **109**: 1112-1126.

Grobelak A, Hiller J. 2017. Bacterial siderophores promote plant growth: Screening of catechol and hydroxamate siderophores. *International Journal of Phytoremediation* **19**(9): 825-833.

Gruber S, Seidl-Seiboth V. 2012. Self versus non-self: fungal cell wall degradation in *Trichoderma*. *Microbiology-Sgm* **158**: 26-34.

Guthrie JL, Castle AJ. 2006. Chitinase production during interaction of *Trichoderma aggressivum* and *Agaricus bisporus*. *Canadian Journal of Microbiology* **52**(10): 961-967.

Haas D, Defago G. 2005. Biological control of soil-borne pathogens by fluorescent pseudomonads. *Nature Reviews Microbiology* **3**(4): 307-319.

Halecker S, Wennrich JP, Rodrigo S, Andrée N, Rabsch L, Baschien C, Steinert M, Stadler M, Surup F, Schulz B. 2020. Fungal endophytes for biocontrol of ash dieback: the antagonistic potential of *Hypoxylon rubiginosum*. *Fungal ecology.* **45**: 100918

Hardoim PR, van Overbeek LS, Berg G, Pirttila AM, Compant S, Campisano A, Doring M, Sessitsch A. 2015. The hidden world within plants: Ecological and evolutionary considerations for defining functioning of microbial endophytes. *Microbiology and Molecular Biology Reviews* **79**(3): 293-320.

Haselwandter K, Winkelmann G 2007. Siderophores of Symbiotic Fungi. In: Varma A, Chincholkar SB eds. *Microbial Siderophores*. Berlin, Heidelberg: Springer Berlin Heidelberg, 91-103.

Huang WY, Cai YZ, Xing J, Corke H, Sun M. 2007. A potential antioxidant resource: Endophytic fungi from medicinal plants. *Economic Botany* **61**(1): 14-30.

Hubbes M. 2008. Induced resistance for the control of Dutch elm disease. *Investigación agraria. Sistemas y recursos forestales, ISSN 1131-7965, Vol. 13, Nº 1, 2004, pp. 185-196*.

Hueck CJ. 1998. Type III protein secretion systems in bacterial pathogens of animals and plants. *Microbiology and Molecular Biology Reviews* **62**(2): 379-433.

Joubert PM, Doty SL. 2018. Endophytic Yeasts: Biology, Ecology and Applications. *Endophytes of Forest Trees: Biology and Applications, 2nd Edition* **86**: 3-14.

Jumpponen A, Trappe JM. 1998. Dark septate endophytes: a review of facultative biotrophic root-colonizing fungi. *New Phytologist* **140**(2): 295-310.

Kalogiannis S, Tjamos SE, Stergiou A, Antoniou PP, Ziogas BN, Tjamos EC. 2006. Selection and evaluation of phyllosphere yeasts as biocontrol agents against grey mould of tomato.

European Journal of Plant Pathology **116**(1): 69-76.

Kandel SL, Firrincieli A, Joubert PM, Okubara PA, Leston ND, McGeorge KM, Mugnozza GS, Harfouche A, Kim SH, Doty SL. 2017. An *In vitro* study of bio-control and plant growth promotion potential of Salicaceae endophytes. *Frontiers in Microbiology* **8**: 16.

Khan AL, Hamayun M, Kang S-M, Kim Y-H, Jung H-Y, Lee J-H, Lee I-J. 2012. Endophytic fungal association via gibberellins and indole acetic acid can improve plant growth under abiotic stress: an example of *Paecilomyces formosus* LHL10. *Bmc Microbiology* **12:** 3.

Khan SA, Hamayun M, Kim H-Y, Yoon H-J, Lee I-J, Kim J-G. 2009. Gibberellin production and plant growth promotion by a newly isolated strain of *Gliomastix murorum*. *World Journal of Microbiology and Biotechnology* **25**(5): 829-833.

Khare E, Mishra J, Arora NK. 2018. Multifaceted interactions between endophytes and plant: developments and prospects. *Frontiers in Microbiology* **9:** 2732.

Krings M, Taylor TN, Hass H, Kerp H, Dotzler N, Hermsen EJ. 2007. Fungal endophytes in a 400-million-yr-old land plant: infection pathways, spatial distribution, and host responses. *New Phytologist* **174**(3): 648-657.

Kumar P, Thakur S, Dhingra GK, Singh A, Pal MK, Harshvardhan K, Dubey RC, Maheshwari DK. 2018. Inoculation of siderophore producing rhizobacteria and their consortium for growth enhancement of wheat plant. *Biocatalysis and Agricultural Biotechnology* **15**: 264-269.

Kusari P, Kusari S, Spiteller M, Kayser O. 2013. Endophytic fungi harbored in *Cannabis sativa* L.: diversity and potential as biocontrol agents against host plant-specific phytopathogens. *Fungal Diversity* **60**(1): 137-151.

Lata R, Chowdhury S, Gond SK, White JF, Jr. 2018. Induction of abiotic stress tolerance in plants by endophytic microbes. *Letters in Applied Microbiology* **66**(4): 268-276.

Laurentin A, Edwards CA. 2003. A microtiter modification of the anthrone-sulfuric acid colorimetric assay for glucose-based carbohydrates. *Analytical Biochemistry* **315**(1):

143-145.

Lee HB, Magan N. 1999. Environmental factors and nutritional utilization patterns affect niche overlap indices between *Aspergillus ochraceus* and other spoilage fungi. *Letters in Applied Microbiology* **28**(4): 300-304.

Li M, Lopez R, Venturas M, Martín JA, Dominguez J, González-Gordaliza G, Gil L and Rodriguez-Calcerrada J. 2016. Physiological and biochemical differences among *Ulmus minor* genotypes showing a gradient of resistance to Dutch elm disease. Forest Pathology. **46**(3):215-228.

Malinowski DP, Belesky DP. 2000. Adaptations of endophyte-infected cool-season grasses to environmental stresses: Mechanisms of drought and mineral stress tolerance. *Crop Science* **40**(4): 923-940.

Malmierca MG, Cardoza RE, Alexander NJ, McCormick SP, Hermosa R, Monte E, Gutierrez S. 2012. Involvement of *Trichoderma* trichothecenes in the Biocontrol Activity and Induction of Plant Defense-Related Genes. *Applied and Environmental Microbiology* **78**(14): 4856-4868.

Mancera-López ME, Izquierdo-Estevez WF, Escalante-Sanchez A, Ibarra JE, Barrera-Cortes J. 2019. Encapsulation of *Trichoderma harzianum* conidia as a method of conidia preservation at room temperature and propagation in submerged culture. *Biocontrol Science and Technology* **29**(2): 107-130.

Maness N 2010. Extraction and analysis of soluble carbohydrates. In: Sunkar R ed. *Plant Stress Tolerance: Methods and Protocols*. Totowa: Humana Press Inc, 341-370.

Martín JA, Macaya-Sanz D, Witzell J, Blumenstein K, Gil L. 2015. Strong *in vitro* antagonism by elm xylem endophytes is not accompanied by temporally stable in planta protection against a vascular pathogen under field conditions. *European Journal of Plant Pathology* **142**(1): 185-196.

Martín JA, Solla A, Witzell J, Gil L, Garcia-Vallejo MC. 2010. Antifungal effect and reduction of

Ulmus minor symptoms to *Ophiostoma novo-ulmi* by carvacrol and salicylic acid. *European Journal of Plant Pathology* **127**(1): 21-32.

Martín JA, Witzell J, Blumenstein K, Rozpedowska E, Helander M, Sieber TN, Gil L. 2013. Resistance to Dutch Elm Disease reduces presence of xylem endophytic fungi in elms (*Ulmus* spp.). *Plos One* **8**(2): 13.

Martín JA, Sobrino-Plata J, Rodríguez-Calcerrada J, Collada C, Gil L. 2019. Breeding and scientific advances in the fight against Dutch elm disease: Will they allow the use of elms in forest restoration? *New Forests* **50**(2): 183-215.

Martínez-Álvarez P, Arcadio Fernández-González R, Vicente Sanz-Ros A, Pando V, Diez JJ. 2016. Two fungal endophytes reduce the severity of pitch canker disease in *Pinus radiata* seedlings. *Biological Control* **94**: 1-10.

Martínez-Arias C, Macaya-Sanz D, Witzell J, Martín JA. 2019. Enhancement of *Populus alba* tolerance to *Venturia tremulae* upon inoculation with endophytes showing in vitro biocontrol potential. *European Journal of Plant Pathology* **153**(4): 1031-1042.

Mayerhofer HJ, Marshall RT, White CH, Lu M. 1973. Characterization of a heat-stable protease of *Pseudomonas fluorescens* P26. *Applied Microbiology* **25**(1): 44-48.

Mejía LC, Rojas EI, Maynard Z, Van Bael S, Arnold AE, Hebbar P, Samuels GJ, Robbins N, Herre EA. 2008. Endophytic fungi as biocontrol agents of *Theobroma cacao* pathogens. *Biological Control* **46**(1): 4-14.

Millar RL, Higgins VJ. 1970. Association of cyanide with infection of birdsfoot trefoil by *Stemphylium loti*. *Phytopathology* **60**(1): 104-110.

Mishra A, Singh SP, Mahfooz S, Singh SP, Bhattacharya A, Mishra N, Nautiyal CS. 2018. Endophyte-mediated modulation of defense-related genes and systemic resistance in *Withania somnifera* (L.) dunal under *Alternaria alternate* stress. *Applied and Environmental Microbiology* **84**(8): e02845-02817.

Moricca S, Ginetti B, Ragazzi A. 2012. Species- and organ-specificity in endophytes colonizing

healthy and declining Mediterranean oaks. *Phytopathologia Mediterranea* **51**(3): 587-598.

Möller B, Weijers D. 2009. Auxin Control of Embryo Patterning. *Cold Spring Harbor perspectives in biology* **1**: a001545.

Naznin HA, Kiyohara D, Kimura M, Miyazawa M, Shimizu M, Hyakumachi M. 2014. Systemic Resistance Induced by Volatile Organic Compounds Emitted by Plant Growth-Promoting Fungi in *Arabidopsis thaliana*. *Plos One* **9**(1).

Nutaratat P, Srisuk N, Arunrattiyakorn P, Limtong S. 2014. Plant growth-promoting traits of epiphytic and endophytic yeasts isolated from rice and sugar cane leaves in Thailand. *Fungal Biology* **118**(8): 683-694.

Oide S, Moeder W, Krasnoff S, Gibson D, Haas H, Yoshioka K, Turgeon BG. 2006. NPS6, encoding a nonribosomal peptide synthetase involved in siderophore-mediated iron metabolism, is a conserved virulence determinant of plant pathogenic ascomycetes. *Plant Cell* **18**(10): 2836-2853.

Orlandelli RC, de Almeida TT, Alberto RN, Polonio JC, Azevedo JL, Pamphile JA. 2015. Antifungal and proteolytic activities of endophytic fungi isolated from *Piper hispidum* Sw. *Brazilian Journal of Microbiology* **46**(2): 359-366.

Oteino N, Lally RD, Kiwanuka S, Lloyd A, Ryan D, Germaine KJ, Dowling DN. 2015. Plant growth promotion induced by phosphate solubilizing endophytic *Pseudomonas isolates*. *Frontiers in Microbiology* **6:** 745.

Paredes M, Nolasco O, Acuna R, Gutierrez AIF. 2016. Chitinases genes expression of *Beauveria bassiana* against *Fusarium oxysporum* and *Peronospora variabilis* substrates. *Scientia Agropecuaria* **7**(3): 239-244.

Passari AK, Mishra VK, Gupta VK, Yadav MK, Saikia R, Singh BP. 2015. *In Vitro* and *In Vivo* plant growth promoting activities and DNA fingerprinting of antagonistic endophytic actinomycetes associates with medicinal plants. *Plos One* **10**(9).

Patten CL, Glick BR. 2002. Role of *Pseudomonas putida* indoleacetic acid in development of the host plant root system. *Applied and Environmental Microbiology* **68**(8): 3795-3801.

Pieterse CMJ, Zamioudis C, Berendsen RL, Weller DM, Van Wees SCM, Bakker P. 2014. Induced systemic resistance by beneficial microbes. *Annual Review of Phytopathology, Vol 52* **52**: 347-375.

Postma J, Goossen-van de Geijn H. 2016. Twenty-four years of Dutch Trig(R) application to control Dutch elm disease. *Biocontrol* **61**(3): 305-312.

Punja ZK, Utkhede RS. 2003. Using fungi and yeasts to manage vegetable crop diseases. *Trends in Biotechnology* **21**(9): 400-407.

Qawasmeh A, Obied HK, Raman A, Wheatley W. 2012. Influence of fungal endophyte infection on phenolic content and antioxidant activity in grasses: Interaction between *Lolium perenne* and different strains of *Neotyphodium lolii*. *Journal of Agricultural and Food Chemistry* **60**(13): 3381-3388.

Rabiey M, Hailey LE, Roy SR, Grenz K, Al-Zadjali MAS, Barret GA, Jackson RW. 2019. Endophytes vs tree pathogens and pests: can they be used as biological control agents to improve tree health? *European Journal of Plant Pathology*.

Radzki W, Gutierrez Manero FJ, Algar E, Lucas Garcia JA, Garcia-Villaraco A, Ramos Solano B. 2013. Bacterial siderophores efficiently provide iron to iron-starved tomato plants in hydroponics culture. *Antonie Van Leeuwenhoek International Journal of General and Molecular Microbiology* **104**(3): 321-330.

Redman RS, Freeman S, Clifton DR, Morrel J, Brown G, Rodriguez RJ. 1999. Biochemical analysis of plant protection afforded by a nonpathogenic endophytic mutant of *Colletotrichum magna*. *Plant Physiology* **119**(2): 795-804.

Redman RS, Kim YO, Woodward C, Greer C, Espino L, Doty SL, Rodriguez RJ. 2011. Increased fitness of rice plants to abiotic stress via habitat adapted symbiosis: A strategy for mitigating impacts of climate change. *Plos One* **6**(7).

Rho T, Kim SH. 2017. Endophyte effects on photosynthesis and water use of plant hosts: A meta-analysis. *Functional Importance of the Plant Microbiome: Implications for Agriculture, Forestry and Bioenergy*: 43-69.

Rijavec T, Lapanje A. 2016. Hydrogen cyanide in the rhizosphere: not suppressing plant pathogens, but rather regulating availability of phosphate. *Frontiers in Microbiology* **7**: 1785.

Rodriguez RJ, White JF, Jr., Arnold AE, Redman RS. 2009. Fungal endophytes: diversity and functional roles. *New Phytologist* **182**(2): 314-330.

Rosa M, Prado C, Podazza G, Interdonato R, Gonzalez JA, Hilal M, Prado FE. 2009. Soluble sugars metabolism, sensing and abiotic stress. A complex network in the life of plants. *Plant Signaling and Behavior* **4**(5): 388-393.

Roy S, Banerjee D. 2019. Volatile organic compounds from endophytic fungi. *Recent Advancement in White Biotechnology through Fungi, Vol 2: Perspective for Value-Added Products and Environments*: 149-175.

Ryu CM, Farag MA, Hu CH, Reddy MS, Kloepper JW, Pare PW. 2004. Bacterial volatiles induce systemic resistance in Arabidopsis. *Plant Physiology* **134**(3): 1017-1026.

Scheffer RJ. 1990. MECHANISMS INVOLVED IN BIOLOGICAL-CONTROL OF DUTCH ELM DISEASE. *Journal of Phytopathology-Phytopathologische Zeitschrift* **130**(4): 265-276.

Schelfer RJ, Voeten JGWF, Guries RP. 2008. Biological control of dutch elm disease. *Plant Disease* **92**(2): 192-200.

Schulz B, Boyle C. 2005. The endophytic continuum. *Mycological Research* **109**: 661-686.

Schwyn B, Neilands JB. 1987. Universal chemical assay for the detection and determination of siderophores. *Analytical Biochemistry* **160**(1): 47-56.

Sen D, Paul K, Saha C, Mukherjee G, Nag M, Ghosh S, Das A, Seal A, Tripathy S. 2019. A unique life-strategy of an endophytic yeast *Rhodotorula mucilaginosa* JGTA-S1-a comparative genomics viewpoint. *DNA Research* **26**(2): 131-146.

Senthilkumar M, Swarnalakshmi K, Govindasamy V, Lee YK, Annapurna K. 2009. Biocontrol potential of soybean bacterial endophytes against charcoal rot fungus, *Rhizoctonia bataticola*. *Current Microbiology* **58**(4): 288-293.

Shi Y, Lou K, Li C. 2009. Promotion of plant growth by phytohormone-producing endophytic microbes of sugar beet. *Biology and Fertility of Soils* **45**(6): 645-653.

Silambarasan S, Logeswari P, Cornejo P, Abraham J, Valentine A. 2019. Simultaneous mitigation of aluminum, salinity and drought stress in *Lactuca sativa* growth via formulated plant growth promoting *Rhodotorula mucilaginosa* CAM4. *Ecotoxicology and Environmental Safety* **180**: 63-72.

Solla A, Gil L. 2003. Evaluating *Verticillium dahliae* for biological control of *Ophiostoma novo-ulmi* in *Ulmus minor*. *Plant Pathology* **52**(5): 579-585.

Solla A, Martín JA, Ouellette GB, Gil L. 2005. Influence of plant age on symptom development in *Ulmus minor* following inoculation by *Ophiostoma novo-ulmi. Plant Disease* **89**(10): 1035-1040.

Sudhadham M, Prakitsin S, Sivichai S, Chaiyarat R, Dorrestein GM, Menken SBJ, de Hoog GS. 2008. The neurotropic black yeast Exophiala dermatitidis has a possible origin in the tropical rain forest. Studies in Mycology (61): 145-155.

Tchernoff V. 1965. Methods for screening and for the rapid selection of elms for resistance to Dutch Elm Disease. *Acta Botanica Neerlandica* **14**(4): 409-452.

Toju H, Peay KG, Yamamichi M, Narisawa K, Hiruma K, Naito K, Fukuda S, Ushio M, Nakaoka S, Onoda Y, et al. 2018. Core microbiomes for sustainable agroecosystems. *Nature Plants* **4**(5): 247-257.

Udvardi MK, Czechowski T, Scheible W-R. 2008. Eleven golden rules of quantitative RT-PCR. *Plant Cell* **20**(7): 1736-1737.

Verma VC, Singh SK, Prakash S. 2011. Bio-control and plant growth promotion potential of siderophore producing endophytic *Streptomyces* from *Azadirachta indica* A. Juss.

Journal of Basic Microbiology **51**(5): 550-556.

Verslues PE, Sharma S. 2010. Proline metabolism and its implications for plant-environment interaction. *The arabidopsis book* **8**: e0140-e0140.

Videira SS, de Oliveira DM, de Morais RF, Borges WL, Divan Baldani VL, Baldani JI. 2012. Genetic diversity and plant growth promoting traits of diazotrophic bacteria isolated from two *Pennisetum purpureum* Schum. genotypes grown in the field. *Plant and Soil* **356**(1-2): 51-66.

Vinale F, Sivasithamparam K, Ghisalberti EL, Marra R, Barbetti MJ, Li H, Woo SL, Lorito M. 2008. A novel role for *Trichoderma* secondary metabolites in the interactions with plants. *Physiological and Molecular Plant Pathology* **72**(1-3): 80-86.

Wei Z, Yang TJ, Friman VP, Xu YC, Shen QR, Jousset A. 2015. Trophic network architecture of root-associated bacterial communities determines pathogen invasion and plant health. *Nature Communications* **6**: 8417.

White JF, Jr., Torres MS. 2010. Is plant endophyte-mediated defensive mutualism the result of oxidative stress protection? *Physiologia Plantarum* **138**(4): 440-446.

White TJ, Bruns T, Lee S, Taylor JW 1990. Amplification and direct sequencing of fungal ribosomal RNA genes for phylogenetics. *PCR protocols: A guide to methods and applications*. NewYork, 315-322.

Witzell J, Martín JA. 2008. Phenolic metabolites in the resistance of northern forest trees to pathogens - past experiences and future prospects. *Canadian Journal of Forest Research-Revue Canadienne De Recherche Forestière* **38**(11): 2711-2727.

Witzell J, Martín JA. 2018. Endophytes and Forest Health. *Endophytes of Forest Trees: Biology and Applications, 2nd Edition* **86**: 261-282.

Wonglom P, Ito S, Sunpapao A. 2020. Volatile organic compounds emitted from endophytic fungus *Trichoderma asperellum* T1 mediate antifungal activity, defense response and promote plant growth in lettuce (*Lactuca sativa*). *Fungal Ecology* **43**: 100867

Xin G, Glawe D, Doty SL. 2009. Characterization of three endophytic, indole-3-acetic acid-producing yeasts occurring in Populus trees. *Mycological Research* **113**: 973-980.

Yang MZ, Ma MD, Yuan MQ, Huang ZY, Yang WX, Zhang HB, Huang LH, Ren AY, Shan H. 2016. Fungal endophytes as a metabolic fine-tuning regulator for wine grape. *Plos One* **11**(9).

Zhang D, Spadaro D, Valente S, Garibaldi A, Gullino ML. 2012. Cloning, characterization, expression and antifungal activity of an alkaline serine protease of *Aureobasidium pullulans* PL5 involved in the biological control of postharvest pathogens. *International Journal of Food Microbiology* **153**(3): 453-464.

Zhang F, Yang X, Ran W, Shen Q. 2014. *Fusarium oxysporum* induces the production of proteins and volatile organic compounds by *Trichoderma harzianum* T-E5. *Fems Microbiology Letters* **359**(1): 116-123.

Table and Figure captions

Table 1: Fungal treatment and plant material specifications. E-O-: control plants without endophyte or *O. novo-ulmi*, E+O-: endophyte-treated plants without *O. novo-ulmi*, E-O+: *O. novo-ulmi*-treated plants without previous endophyte treatment, E+O+: endophyte- and *O. novo-ulmi*-treated plants.

Table 2: Top three BLAST hits (based on nucleotide megablast of ITS rDNA sequences) with corresponding GenBank taxa identity and NCBI accession number.

Table 3: Protease and chitinase activities, siderophore and hydrogen cyanide production, and phosphate solubilisation in *in vitro* assays of the fungal endophytes and the pathogen at the end of the experiment (day 20). Different letters in the same row indicate significant differences between fungi, according to Fisher's post-hoc test ($P<0.05$).

Fig. 1: *In vitro* interactions between *O. novo-ulmi* and fungal endophytes. (A) *O. novo-ulmi* growth when confronted against fungal endophytes in dual *in vitro* plate assays; (B) *O. novo-ulmi* growth when confronted "mouth-to-mouth" with fungal endophytes in petri dishes to evaluate the effect of endophyte volatile substances (VOCs) emission**;** (C) *O. novo-ulmi* growth in the presence of endophyte liquid filtrates in microplates**.** In (C) *O. novo-ulmi*, growth is measured by optical density (OD). Asterisks indicate statistically significant differences with the control treatment according to Fisher's post-hoc test ($P<0.05$).

Fig. 2: Two-joining clustering analysis of the in-house configured phenotypic arrays of fungal endophytes and *O. novo-ulmi* (horizontal axis) growing with different nutrients and inhibitory substrates (vertical axis). Euclidean distances were used in the clustering of fungal endophytes and substrates. The colour legend indicates inhibition (bluish colours) or promotion (reddish colours) of fungal growth.

Fig. 3: Indole-3-acetic acid (IAA) and gibberellic acid (GA_3) production by fungal endophytes and pathogen. (A) IAA production by *O. novo-ulmi* and fungal endophytes (YCB36, P5 and YM11) after 15 days of incubation in malt extract broth containing 0.2 % L-tryptophan. **(B)** GA_3 content in liquid filtrates of *O. novo-ulmi* and the three endophytes growing in YMG for 40 days. Different letters indicate significant differences between fungi according to Fisher's post-hoc test (P<0.05).

Fig. 4: Leaf wilting induced by *O. novo-ulmi* inoculation at 30, 60, 120 dpi and 1 ypi in: P5+YM11-treated trees **(A),** and YCB36-treated trees **(C).** The proportion of trees with leaf wilting percentages higher or lower than 50% is shown in (**B)** for P5+YM11-treatment and in (**D)** for YCB36-treatment. E-O+ indicates non-endophyte-treated trees with *O. novo-ulmi* inoculation, and E+O+ indicates endophyte-treated trees with *O. novo-ulmi* inoculation**.** Non-*O. novo-ulmi*-inoculated trees (not shown) showed no wilting symptoms. Asterisks in graphs (A) and (B) indicate significant differences between treatments according to Fisher's post-hoc test (P<0.05).

Fig. 5: Stomatal conductance measured at 0 dpi and 30 dpi in P5+YM11-treated plants **(A)** and YCB36-treated plants **(B).** Treatments were: trees without endophyte or *O. novo-ulmi* inoculation (E-O-); non-endophyte-treated trees with *O. novo-ulmi* inoculation (E-O+); endophyte-treated trees without *O. novo-ulmi* inoculation (E+O-), and trees treated with endophyte before *O. novo-ulmi* inoculation (E+O+). Different letters indicate significant differences between treatments according to Fisher's post-hoc test (P<0.05).

Fig. 6: Relative presence of fungal endophytes estimated by qPCR at 75 dpi **(A)** and 1 ypi **(B)** in P5+YM11-treated trees (left panel) and YCB36 treated trees (right panel) (E-O-). Quantifications were performed at 5 and 50 cm above the endophyte inoculation point. Results are shown as a fold change of presence in non-endophyte inoculated trees (E-O-). Asterisks indicate significant differences with E-O- trees according to Fisher's post-hoc test (P<0.05).

Fig. 7: Biochemical measurements in wood samples of YCB36-treated and control trees at 5 and 50 cm from the inoculation point and at 75 dpi. (A) Total flavonoid content; (**B)** total phenolic content and **(C)** proline content. Different letters in the graphs indicate significant differences between treated and untreated trees at 5 (normal letters) and 50 cm (italics) according to Fisher's post-hoc test (P<0.05).

Fig. S1: Experimental procedure. First, a fungal cell suspension was inoculated into the vascular system at the trunk base using an endotherapy device. *O. novo-ulmi* inoculations were performed 15 days later using a spore suspension, following traditional inoculation methods for DED. Four treatments were applied for each endophyte combination (P5+YM11 or YCB36): E+O-: endophyte-treated plants without *O. novo-ulmi* treatment, E-O+: *O. novo-ulmi*-treated plants without previous endophyte treatment, E+ O+: endophyte and *O. novo-ulmi*-treated plants, and E-O-: non-inoculated plants (neither endophyte nor *O. novo-ulmi*). Leaf wilting was evaluated in each tree at 30, 60, 120 days post (pathogen) inoculation (dpi) and 1 year post-inoculation (ypi) by three independent assessors. At 75 dpi a wood sample was cored with an increment borer (N=3) at 5 and 50 cm above the inoculation point for biochemical and fungal quantification measures. SS = soluble sugars.

Fig. S2: Fungal activities and *O. novo-ulmi* inhibition *in vitro*. Upper panel: protease and chitinase activities and siderophore production in *in vitro* assays performed by fungal endophytes and pathogen at day 20. Dotted red line delimits colony diameter; dotted yellow line delimits clear halo diameter. Chitinase activity and siderophore production were negative (NA) for endophytes P5 and YM11. Lower panel: dual culture and VOC assay results. In the dual

culture, *O. novo-ulmi* (white colony in the left side of the plate) is confronted against fungal endophytes (YCB36, P5 and YM11) (right side of the plate) at day 12. The VOC assay shows the results of *O. novo-ulmi* growth in the presence of endophytes at day 10. The scale bar below each petri dish indicates a length of 1 cm.

Fig. 1

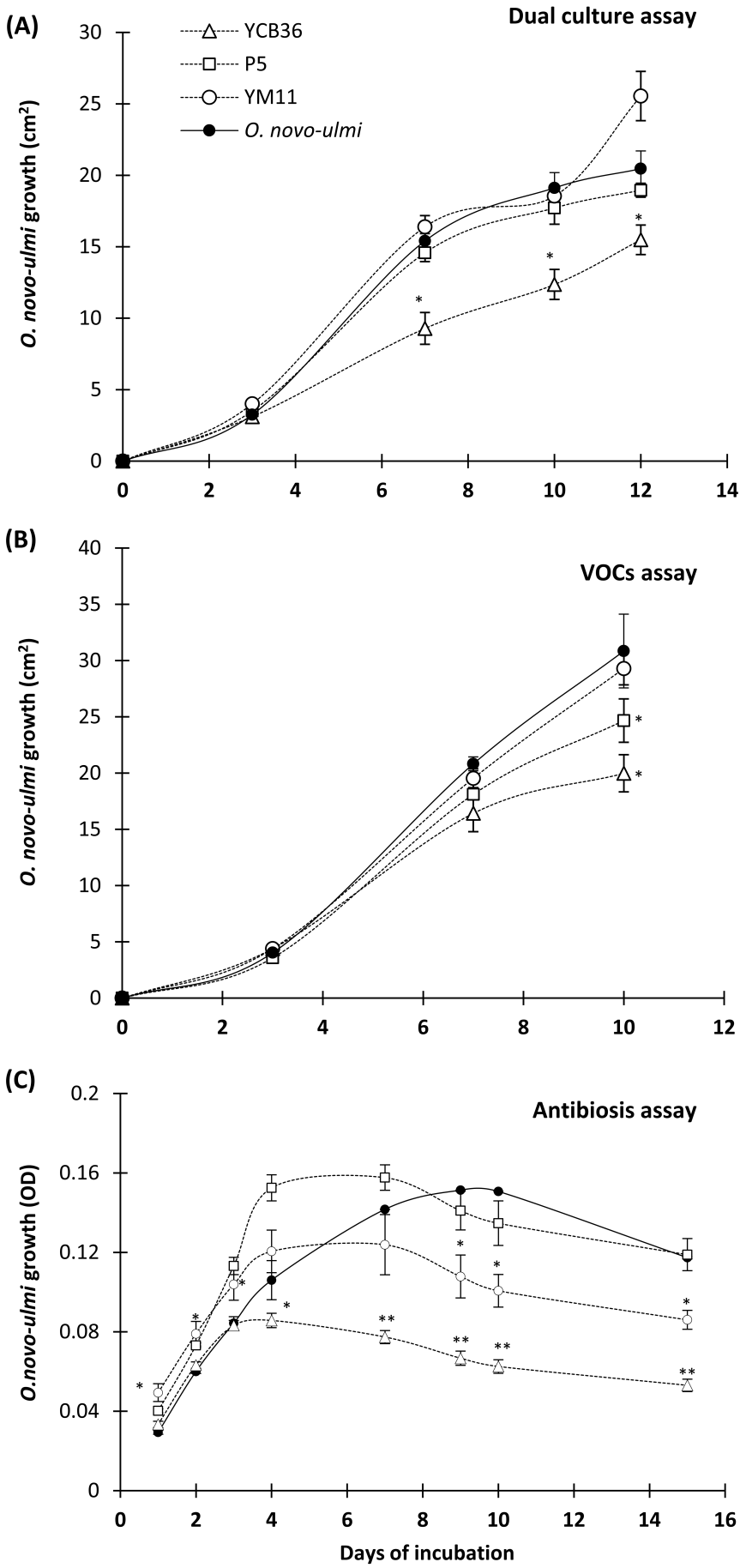
(A)
Dual culture assay
YCB36
P5
YM11
O. novo-ulmi
O. novo-ulmi growth (cm²)
(B)
VOCs assay
O. novo-ulmi growth (cm²)
(C)
Antibiosis assay
O.novo-ulmi growth (OD)
Days of incubation

Fig. 2

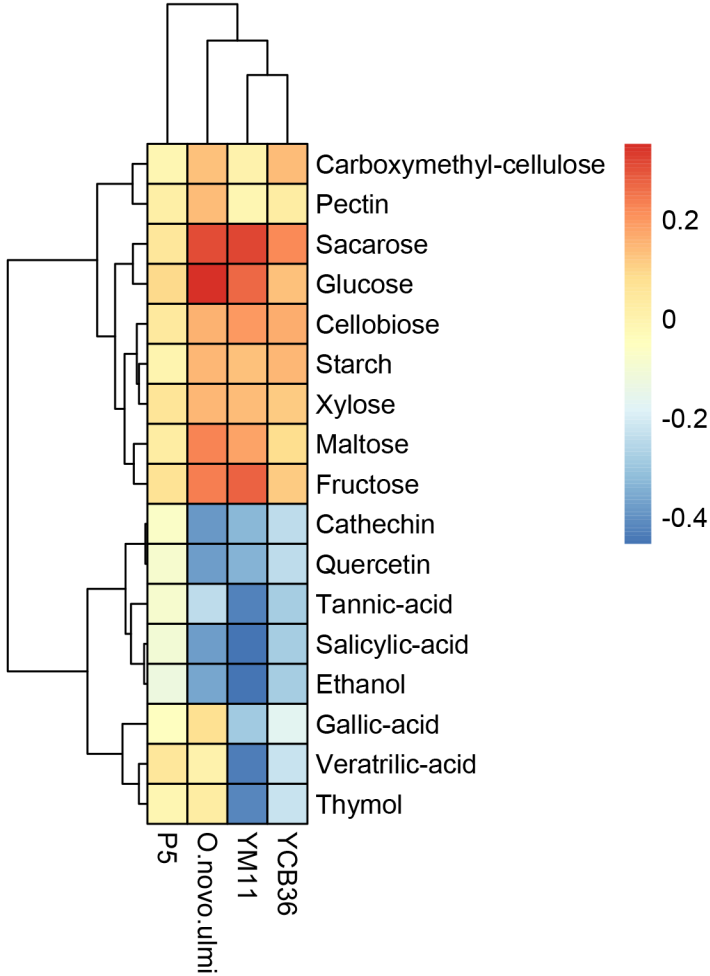
Carboxymethyl-cellulose
Pectin
Sacarose
Glucose
Cellobiose
Starch
Xylose
Maltose
Fructose
Cathechin
Quercetin
Tannic-acid
Salicylic-acid
Ethanol
Gallic-acid
Veratrilic-acid
Thymol
P5
O.novo.ulmi
YM11
YCB36
0.2
0
-0.2
-0.4

Fig. 3

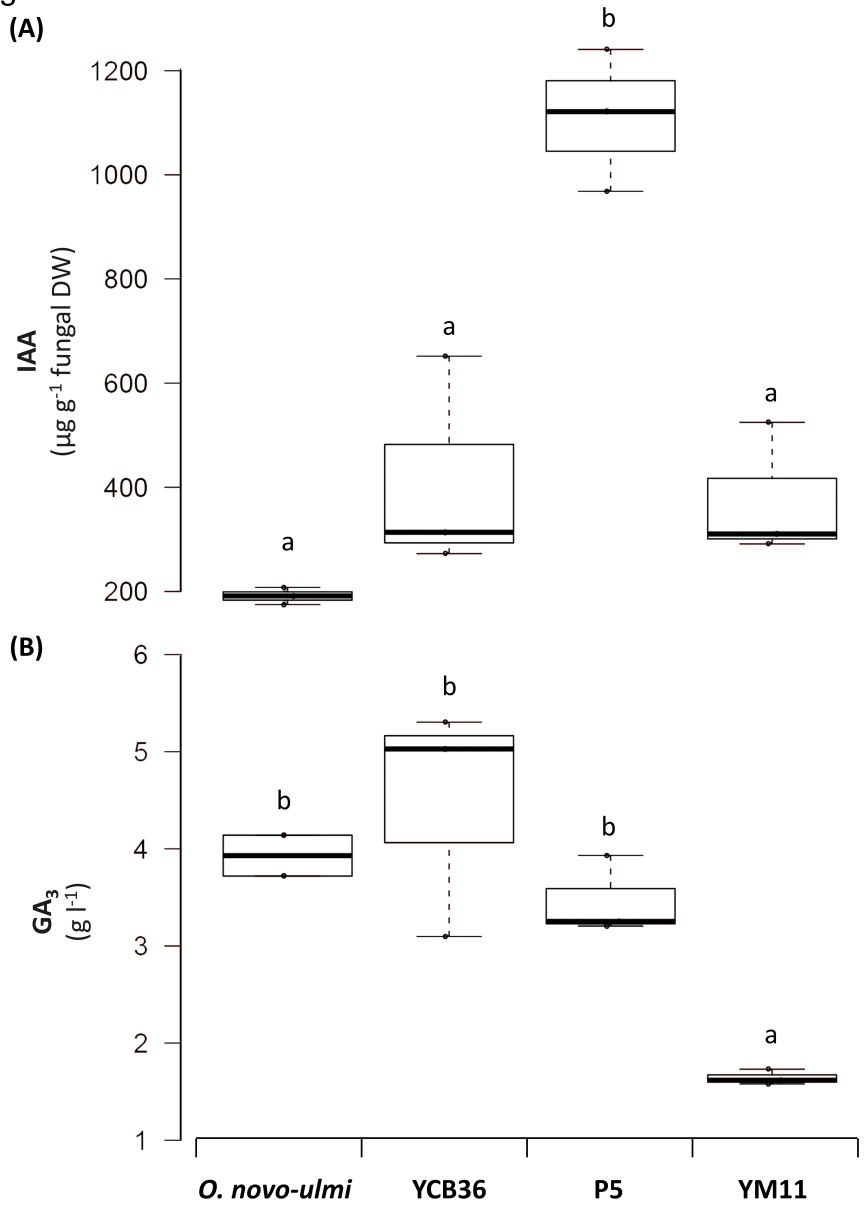
(A)
IAA
(µg g-1 fungal DW)
1200
1000
800
600
400
200
a
a
b
a
(B)
GA3
(g l-1)
6
5
4
3
2
1
b
b
b
a
O. novo-ulmi
YCB36
P5
YM11

Fig. 4

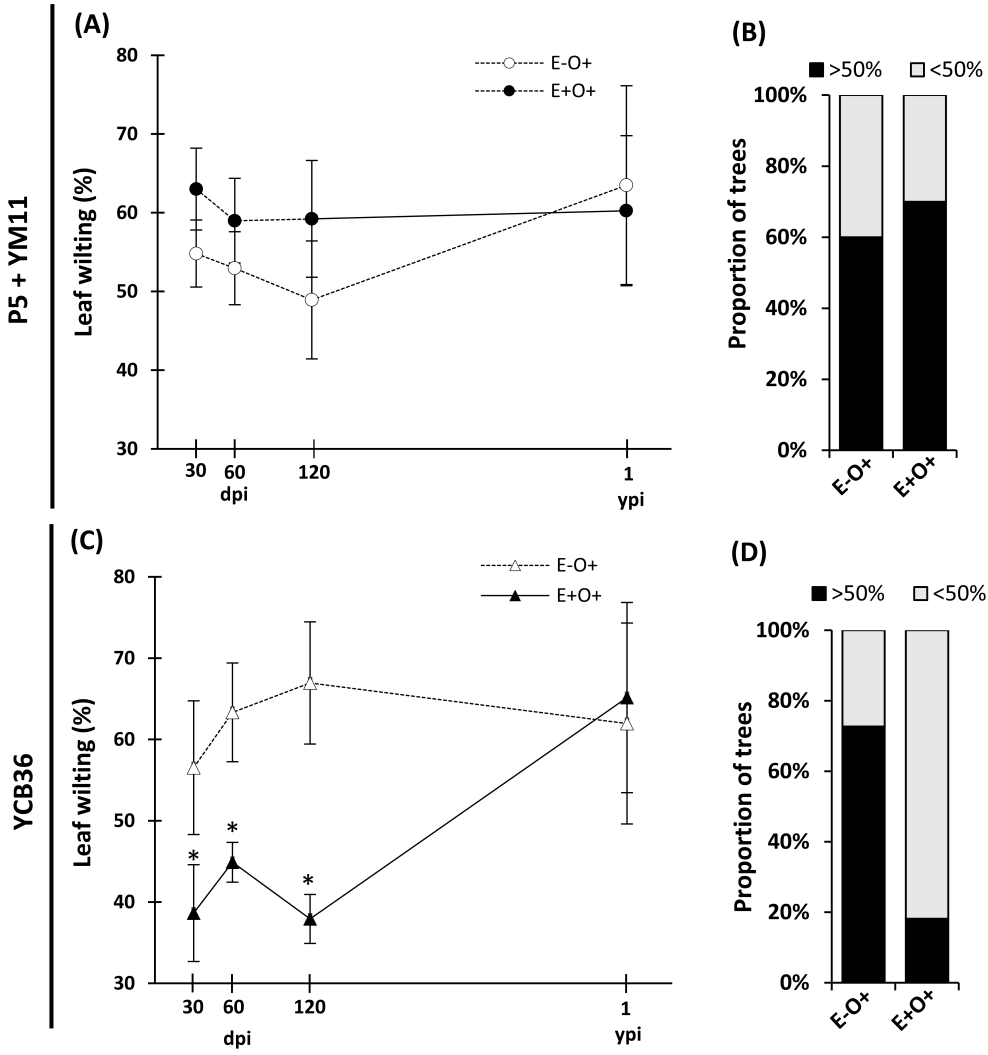
P5 + YM11
(A)
E-O+
E+O+
Leaf wilting (%)
80
70
60
50
40
30
30
60
120
1
dpi
ypi
(B)
>50%
<50%
Proportion of trees
100%
80%
60%
40%
20%
0%
E-O+
E+O+
YCB36
(C)
E-O+
E+O+
Leaf wilting (%)
*
*
*
30
60
120
1
dpi
ypi
(D)
>50%
<50%
Proportion of trees
100%
80%
60%
40%
20%
0%
E-O+
E+O+

Fig. 5

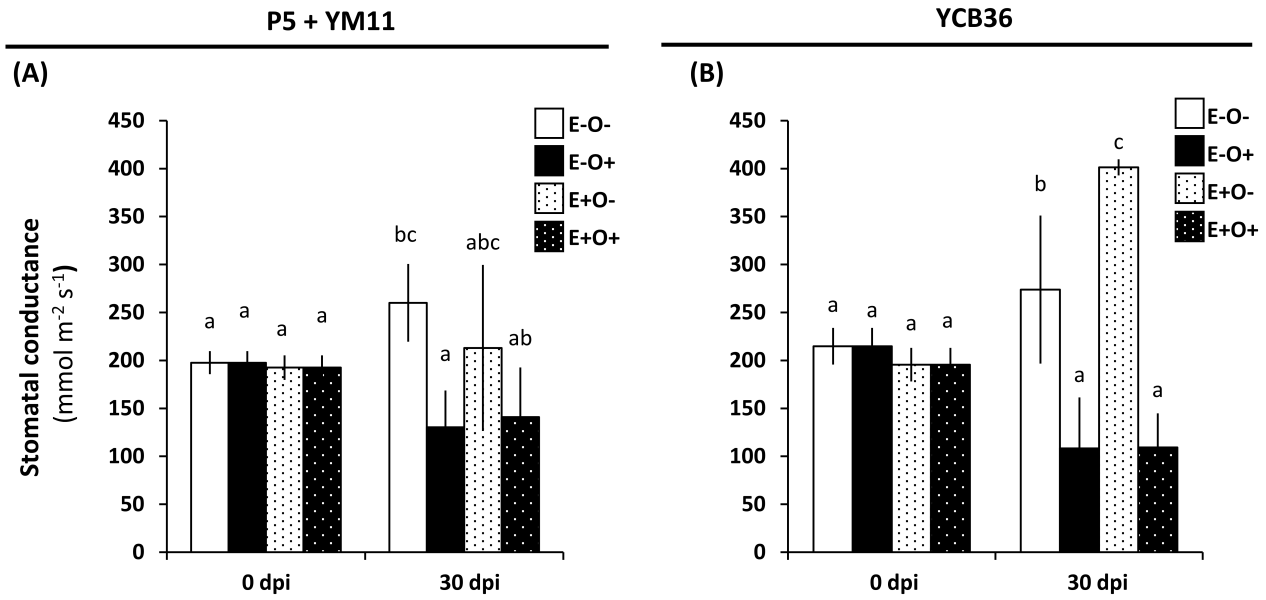
P5 + YM11
(A)
Stomatal conductance
(mmol m-2 s-1)
450
400
350
300
250
200
150
100
50
0
E-O-
E-O+
E+O-
E+O+
a
a
a
a
bc
a
abc
ab
0 dpi
30 dpi
YCB36
(B)
450
400
350
300
250
200
150
100
50
0
E-O-
E-O+
E+O-
E+O+
a
a
a
a
b
a
c
a
0 dpi
30 dpi

Fig. 6

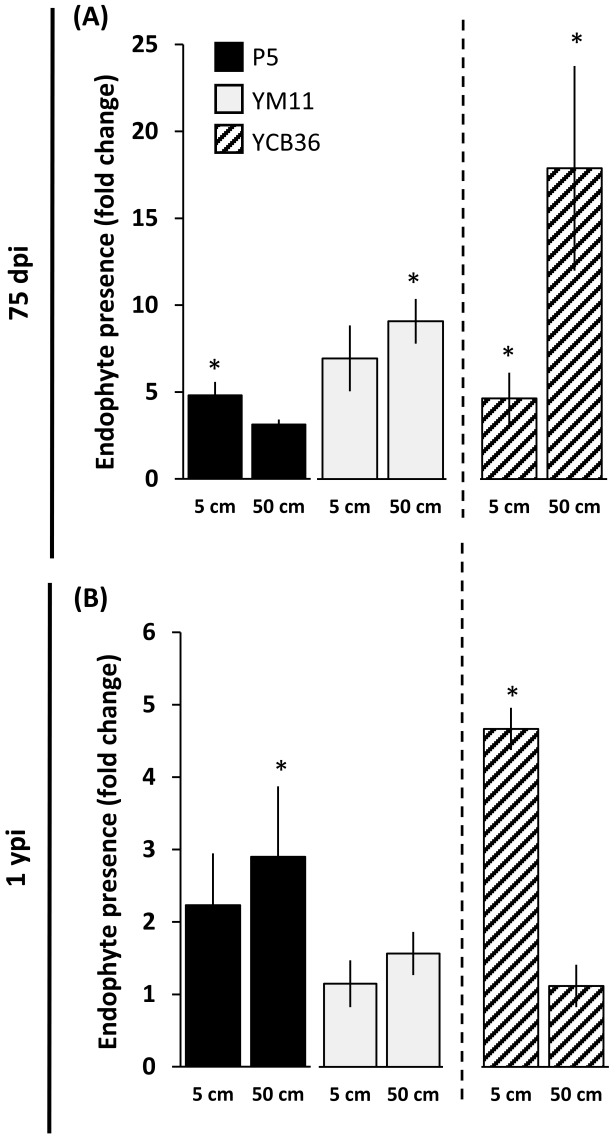
(A)
75 dpi
Endophyte presence (fold change)
25
20
15
10
5
0
P5
YM11
YCB36
*
*
*
*
5 cm
50 cm
5 cm
50 cm
5 cm
50 cm
(B)
1 ypi
Endophyte presence (fold change)
6
5
4
3
2
1
0
*
*
5 cm
50 cm
5 cm
50 cm
5 cm
50 cm

Fig. 7

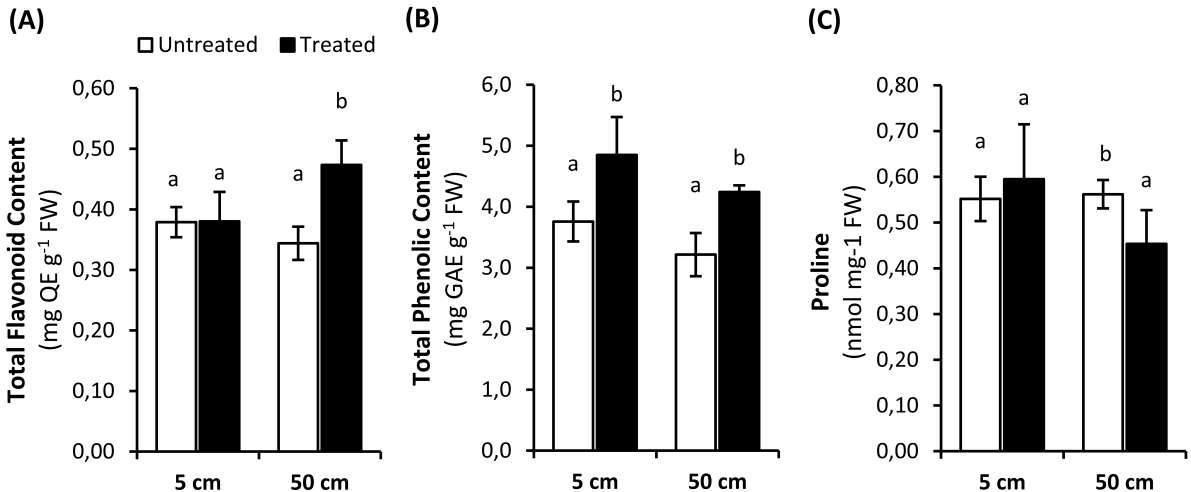
(A)
Untreated
Treated
Total Flavonoid Content
(mg QE g-1 FW)
0,60
0,50
0,40
0,30
0,20
0,10
0,00
a
a
a
b
5 cm
50 cm
(B)
Total Phenolic Content
(mg GAE g-1 FW)
6,0
5,0
4,0
3,0
2,0
1,0
0,0
a
b
a
b
5 cm
50 cm
(C)
Proline
(nmol mg-1 FW)
0,80
0,70
0,60
0,50
0,40
0,30
0,20
0,10
0,00
a
a
b
a
5 cm
50 cm

Table 1: Fungal treatment and plant material specifications. E-O-: control plants without endophyte or *O. novo-ulmi*, E+O-: endophyte-treated plants without *O. novo-ulmi*, E-O+: *O. novo-ulmi*-treated plants without previous endophyte treatment, E+O+: endophyte- and *O. novo-ulmi*-treated plants.

Inoculated endophytes	Plant genotype	DED-tolerance level[1]	Treatment	N
P5+YM11	(M-CC1 × AL-AN1).5	Susceptible	E-O-	5
			E+O-	5
			E-O+	10
			E+O+	10
	(M-CC1 × AL-AN1).7	Susceptible	E-O-	5
			E+O-	5
			E-O+	10
			E+O+	10
	(M-CC1 × AL-AN1).8	Susceptible	E-O-	5
			E+O-	5
			E-O+	10
			E+O+	10
YCB36	(M-CC1 × AL-AN1).15	Susceptible	E-O-	6
			E+O-	12
			E-O+	11
			E+O+	5
---	Sapporo	Highly tolerant	E-O-	8
			E-O+	8
---	M-PZ3	Highly susceptible	E-O-	8
			E-O+	8

[1] According to previous susceptibility tests

Table 2: Top three BLAST hits (based on nucleotide megablast of ITS rDNA sequences) with corresponding GenBank taxa identity and NCBI accession number.

Strain	Description	Max. Score	Total score	Query coverage	E-value	Identities	Gaps	Percentage of identity	Accession NCBI
P5	Cystobasidium	544	544	100	1.00E-150	294/294	0/294	100	LC493223.1
	Cystobasidium	544	544	100	1E-150	294/294	0/294	100	LC493222.1
	Rhodotorula sp.	544	544	100	1E-150	294/295	0/295	100	MK268054.1
YM11	*Exophiala* sp.	1016	1016	94	0	556/562	0/562	99	EU035420.1
	Uncultured fungus	1011	1011	94	0	555/562	0/562	99	FJ820808.1
	Uncultured fungus	996	996	94	0	552/561	1/561	98	KF800433.1
YCB36	Dothideomycetes	1650	1650	87	0	932/951	9/951	98	KX611035.1
	Ascomycota	1639	1639	86	0	926/945	9/945	97.99	KX611067.1
	Phaeosphaeriaceae	1611	1611	84	0	902/916	5/916	98.47	MG208007.1

Table 3: Protease and chitinase activities, siderophore and hydrogen cyanide production, and phosphate solubilisation in *in vitro* assays of the fungal endophytes and the pathogen at the end of the experiment (day 20). Different letters in the same row indicate significant differences between fungi, according to Fisher's post-hoc test ($P<0.05$).

		Fungal strain			
Activity	**Units**	***O. novo-ulmi***	**YCB36**	**P5**	**YM11**
Protease	cm^2 (halo)	28.73 ± 1.96^{c}	10.28 ± 2.48^{b}	1.33 ± 0.06^{a}	5.75 ± 0.71^{b}
Chitinase	cm^2 (halo)	6.46 ± 1.93^{a}	49.85 ± 1.63^{b}	negative	negative
Siderophore	cm^2 (halo)	5.39 ± 0.98^{a}	7.90 ± 0.44^{b}	negative	negative
Hydrogen cyanide	positive/negative	negative	negative	negative	negative
Phosphate solubilization	cm^2 (halo)	negative	negative	negative	negative

Fig. S1

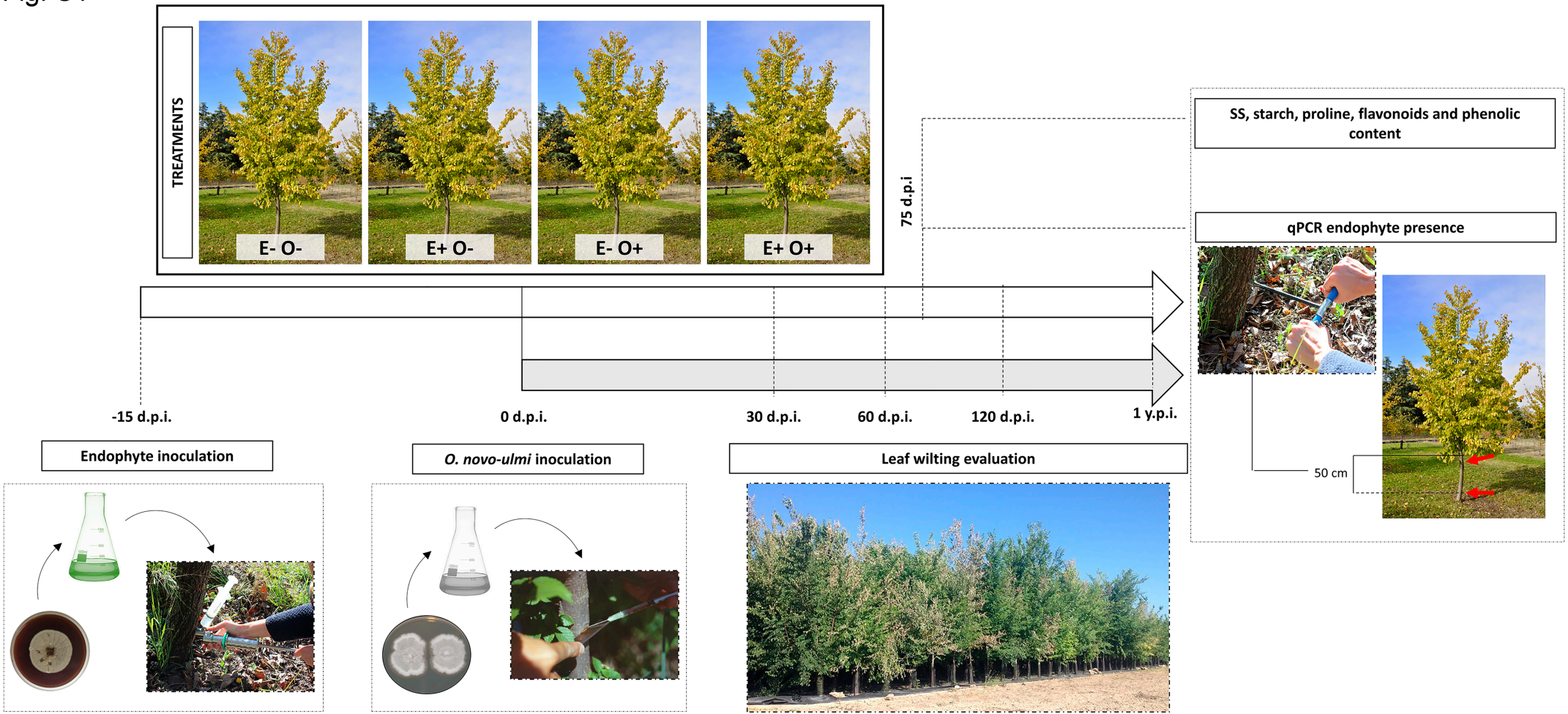
TREATMENTS
E- O-
E+ O-
E- O+
E+ O+
75 d.p.i
SS, starch, proline, flavonoids and phenolic content
qPCR endophyte presence
50 cm
-15 d.p.i.
0 d.p.i.
30 d.p.i.
60 d.p.i.
120 d.p.i.
1 y.p.i.
Endophyte inoculation
O. novo-ulmi inoculation
Leaf wilting evaluation

Fig. S2

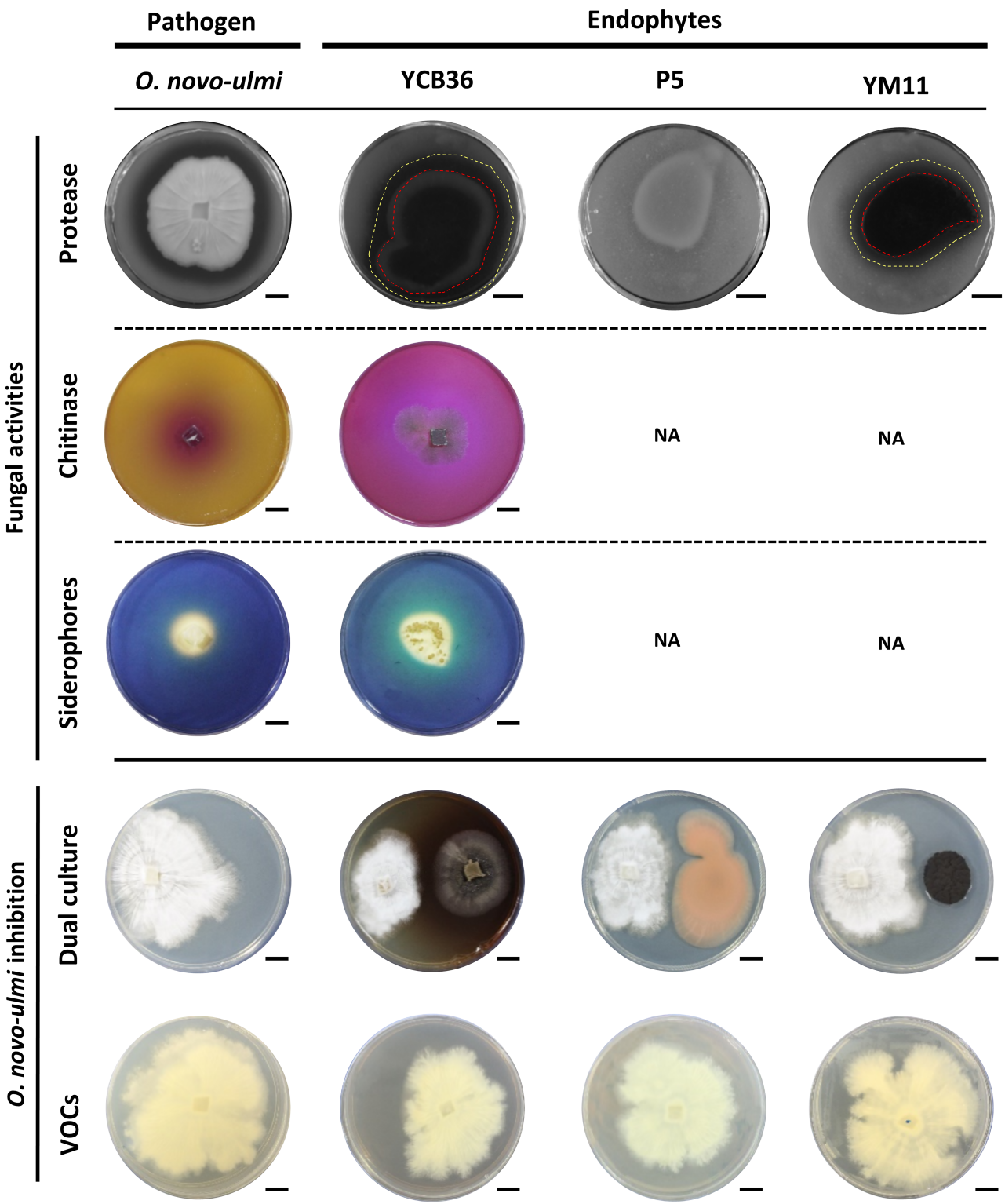
Pathogen
Endophytes
O. novo-ulmi
YCB36
P5
YM11
Fungal activities
Protease
Chitinase
Siderophores
NA
NA
NA
NA
O. novo-ulmi inhibition
Dual culture
VOCs